Quaternary Research

Chronology and glass chemistry of tephra and cryptotephra horizons from lake sediments in northern Alaska, U.S.A.

--Manuscript Draft--

Manuscript Number:	YQRES-D-16-00165R3
Article Type:	Research Paper
Keywords:	Tephra, Tephrochronology, Alaska, Holocene, Brooks Range, Eastern Interior, Aniakchak, Taphonomy
Corresponding Author:	Ali Monteath University of Southampton Southampton, UNITED KINGDOM
First Author:	Ali Monteath
Order of Authors:	Ali Monteath
	Maarten van Hardenbroek
	Lauren Davies
	Duane Froese
	Pete Langdon
	Xiaomei Xu
	Mary Edwards
Abstract:	Holocene tephrostratigraphy in Alaska provides independent chronology and stratigraphic correlation in a region where reworked old (Holocene) organic carbon can significantly distort radiocarbon chronologies. Here we present new glass chemistry and chronology for Holocene tephras preserved in three Alaskan lakes: one in the eastern interior, and two in the southern Brooks Range. Tephra beds in the eastern interior lake-sediment core are correlated with the White River Ash and the Hayes tephra set H (~4200-3700 cal yr BP), while an additional discrete tephra bed is likely from the Aleutian Arc-Alaska Peninsula. Cryptotephras (non-visible tephras) found in the Brooks Range include the informally named "Ruppert tephra" (~2700-2300 cal yr BP), and the Aniakchak caldera-forming event II tephra (CFE II; ~3600 cal yr BP). A third underlying Brooks Range cryptotephra is chemically indistinguishable from the Aniakchak CFE II tephra (4070-3760 cal yr BP) and is likely to be from an earlier eruption of the Aniakchak volcano.

Chronology and glass chemistry of tephra and cryptotephra horizons from lake sediments in northern Alaska, U.S.A.

Alistair J. Monteath [a*], Maarten van Hardenbroek [b], Lauren J. Davies [c], Duane G. Froese [c], Peter G. Langdon [a], Xiaomei Xu [d], Mary E. Edwards [a, e]

[a] *Palaeoecology Laboratory (PLUS), School of Geography, University of Southampton, Southampton SO17 1BJ, UK*

[b] *School of Geography Politics and Sociology, University of Newcastle, Newcastle upon Tyne, NE1 7RU, UK*

[c] *Department of Earth and Atmospheric Sciences, University of Alberta, Edmonton, Alberta T6G 2E3, Canada*

[d] *Keck Carbon Cycle AMS Facility, University of California, Irvine, CA 92697-3100, USA*

[e] *Alaska Quaternary Center, College of Natural Sciences and Mathematics, University of Alaska, Fairbanks, 99775, USA*

Corresponding Author:

Alistair. J. Monteath

Geography and Environment, Room 1067, Shackleton Building 44, University of Southampton, SO17 1BJ

Email: ali.monteath@soton.ac.uk

Phone: 07941778714

Abstract

Holocene tephrostratigraphy in Alaska provides independent chronology and stratigraphic correlation in a region where reworked old (Holocene) organic carbon can significantly distort radiocarbon chronologies. Here we present new glass chemistry and chronology for Holocene tephras preserved in three Alaskan lakes: one in the eastern interior, and two in the southern Brooks Range. Tephra beds in the eastern interior lake-sediment core are correlated with the White River Ash and the Hayes tephra set H (~4200-3700 cal yr BP), while an additional discrete tephra bed is likely from the Aleutian Arc-Alaska Peninsula. Cryptotephras (non-visible tephras) found in the Brooks Range include the informally named “Ruppert tephra” (~2700-2300 cal yr BP), and the Aniakchak caldera-forming event II tephra (CFE II; ~3600 cal yr BP). A third underlying Brooks Range cryptotephra is chemically indistinguishable from the Aniakchak CFE II tephra (4070-3760 cal yr BP) and is likely to be from an earlier eruption of the Aniakchak volcano.

KEYWORDS: Tephra, Tephrochronology, Alaska, Holocene, Brooks Range, Eastern Interior, Aniakchak, Taphonomy

Text (main body)

Introduction

Tephra layers form unique stratigraphic markers that can be used to synchronize and integrate palaeoenvironmental records across a range of terrestrial and marine settings (Lowe, 2011). In particular, studies of cryptotephra (non-visible tephra) have greatly enhanced the application of tephrochronology, and widespread North American tephras are now known to have intercontinental distributions (Coulter *et al.,* 2012; Jensen *et al*., 2014; Zdanowicz *et al.,* 1999).

Alaska is frequently affected by explosive volcanism, including at least eight caldera-forming events during the Holocene (Miller and Smith, 1987), and volcanic ash deposits form widespread stratigraphic markers across much of the state (Riehle, 1985). Current understanding of the Alaska Holocene tephrostratigraphy is largely based on the analysis of discrete visible ash layers and near-source exposures, which are mainly studied to determine eruption frequency and volcanic hazards. However, proximal deposits are commonly removed during subsequent eruptions, and very few regionally extensive and well dated Holocene tephras are known (Davies *et al*., 2016). Despite the value of tephrostratigraphy beyond the extent of these observable volcanic ash beds, the cryptotephra record in Alaska is largely undeveloped with few exceptions (*e.g.,* Payne and Blackford, 2004, 2008; Payne *et al*., 2008; Zander *et al*., 2013). Improving the tephrochronological framework, particularly for interior and northern Alaska, will aid the age modelling and correlation of sedimentary sequences that often lack abundant terrestrial plant macrofossils for ^{14}C-dating (*e.g.,* Abbott and Stafford 1996). Such sequences record palaeoenvironmental features including vegetation responses to climate change (*e.g.,* Brubaker *et al.,* 2005) and the extinction patterns of Pleistocene megafauna (e.g., Guthrie, 2006; Cooper *et al.,* 2015).

Tephra and cryptotephra layers were examined in lake-sediment cores from two areas in Alaska (Fig. 1) as part of a wider project (Lakes and the Arctic Carbon Cycle). Jan Lake in eastern interior Alaska (63°33'53”N, 143°55'1”W) lies downwind of volcanic sources in the Aleutian arc and Alaska Peninsula and preserves two uncorrelated tephra beds dating to 3500-4000 cal yr BP (Carlson and Finney, 2004). Ruppert Lake (67° 4'17”N, 154°14'39”W; see Brubaker *et al*., 1983; Higuera *et al*., 2009) and Woody

Bottom Pond (informal name), hereafter referred to as "WBP" (67°4'33"N, 154°13'53"W), are in the southern Brooks Range. Several late-Quaternary sediment records exist from the Brooks Range (*e.g.,* Edwards et al., 1985; Brubaker *et al*., 1983; Oswald *et al.,* 2012), however, no tephra beds have yet been reported from the region despite its relative proximity to volcanoes producing intercontinental cryptotephra horizons (Mackay *et al.,* 2016). Ruppert Lake and WBP lie within 750 m of each other; however, because Ruppert Lake is much larger (3.1 km^2) than WBP (0.06 km^2) and has inflowing streams (Figure 4), we expected that the sedimentary sequences from Ruppert Lake would contain a higher abundance of volcanic shards (Mangerud, 1984; de Fontaine *et al*., 2007; Pyne O'Donnell, 2011). In order to investigate within-lake variability, we compared a near shore core (RS) and a central (RC) core section from Ruppert Lake.

Methods

Sediment cores were retrieved in July 2013, using a square-rod piston corer (Wright *et al*., 1984). To determine the presence of tephra, amalgamated 5 cm range-finder samples were taken throughout the cores and processed following the stepped floatation methodology of Turney (1998) and Blockley *et al.*, (2005). Where tephra layers were identified additional 1 cm point samples were taken and processed in the same manner to more accurately establish the stratigraphic position of the tephra. Finally, shards were extracted for geochemical analysis following protocols outlined in Blockley *et al.*, (2005).

Glass shards from peak tephra concentrations were first analyzed by electron microprobe (EMPA) at the Department of Earth Sciences, Oxford University, UK, before further analysis by wavelength-dispersive spectrometry (WDS) at the University of Alberta, Canada. Following identification of the Aniakchak caldera-forming eruption II (CFE II) tephra within samples analyzed at Oxford University, Aniakchak CFE II reference material (UA 1602) was run concurrently during analysis at the University of Alberta.

Glass shards were analysed by WDS on the Alberta JEOL 8900 superprobe following established protocols (*e.g.* Jensen *et al*., 2008). Shards were mounted in an epoxy puck and polished to expose internal glass surfaces before being carbon coated prior to EPMA. A standard suite of ten elements (Si, Ti, Al, Fe, Mn, Mg, Ca, Na, K, Cl) were measured using a 10 µm beam with 15 keV accelerating voltage, and 6 nA beam current to minimize Na and K migration during analyses. Two secondary standards of known composition were run concurrently with all volcanic glass samples: i) 3506, Lipari rhyolitic obsidian, and ii) Old Crow tephra, a well-characterized, secondarily hydrated tephra from an unknown source, but possibly derived from the Alaska Peninsula or Aleutian Islands based on chemical composition (Kuehn *et al*., 2011). Results were normalized to 100 % and presented as weight percent (wt %) oxides. New major element chemistry data and associated standard measurements produced at both institutions are reported in supplementary information (Tables S1-S3).

Comparison of the glass chemistry data produced at the University of Oxford and the University of Alberta revealed consistent differences between the analytical totals for some minor elements such as CaO and Cl (supplementary information Table S5, Fig. 1). Differences between Alaska glass populations are often subtle (*e.g.,* Preece *et al*., 2014) and even minor inter-lab variation can complicate interpretation (Kuehn *et al*., 2011). To remove this uncertainty between new volcanic glass data and those of previously analysed samples in the geochemical database at the University of Alberta, data produced at the University of Oxford were excluded from bivariate plots of major and minor element glass chemistry (Figures 3 and 6).

Chronology

New radiocarbon dates derived from plant macrofossils supported the age models presented in Figures 2 and 5. These included eight from WBP, 13 from RC, 10 from RS and two from Jan Lake (supplementary information, Table S4). The two earliest tephra beds in Jan Lake (J118 and J127) were dated on the basis of 22 radiocarbon dates from Carlson and Finney (2004), who described the positions of the two oldest Jan Lake tephras discussed here (supplementary information, Table S4). The youngest Jan Lake tephra was not noted by Carlson and Finney, (2004) and so is only loosely constrained by an age model based on two additional radiocarbon dates from our new sediment core (supplementary information, Table S4). Age models were produced using *Bacon* age modelling software (v.2.2; Blaauw and Christen, 2011), and the Intcal13 calibration data (Reimer *et al.*, 2013). Based on low agreement values, three dates from Jan Lake, one from WBP, one from RS and two from RC were excluded from the age models.

Tephra descriptions, geochemistry and geochronology

Eastern Interior - Jan Lake

Cryptotephra

Volcanic glass was present throughout the Jan Lake core in high concentrations, and three discrete visible tephra beds were noted at 63 cm, 118 cm and 127 cm (Figure 2). The background levels of volcanic glass were too high to identify cryptotephra horizons for large sections of the Jan Lake core, and only two possible cryptotephra layers were targeted for chemical analyses (124 cm and 184 cm). The cryptotephra at 124 cm was found to be chemically indistinguishable from the tephra layer at 127 cm (Figure 3) and likely represents reworking. Glass chemistry analyses from the cryptotephra at 184 cm, produced at the University of Oxford, covered a wide range of compositions suggesting no primary air fall tephra was present (supplementary information, Fig. S2).

Tephra J63

Tephra J63, consists of clear, highly vesicular, blocky, and pumiceous shards, that form a discreet bed <1mm thick. Glass chemistry is composed of a rhyolitic population (72.38 - 75.27 wt% SiO_2) with K_2O

values higher than other tephras observed in Jan Lake (2.97 - 3.24 wt% K_2O; Figure 3). The two sigma modeled age range is 3010-1470 cal yr BP.

Glass chemistry from J63 is similar to the White River Ash tephras originating from Mt Bona-Churchill (Figure 3). The White River Ash tephras are composed of two widespread tephra beds, the White River Ash north (1900 cal yr BP), and the volumetrically larger, White River Ash east (A.D. 833–850) (Lerbekmo, 2008). Although the location and modelled age range of J63 agree better with the White River Ash north, glass chemistry is more similar to the White River Ash east. SiO_2 values of J63 (72.38 - 75.27 wt%) are in close agreement with those found in the White River Ash east (˜72.5 - 76.5 wt%). In contrast, they fall within a common compositional gap spanning 73.5 to 75.9 wt% observed in the White River Ash north, which includes a wider chemical range (71 to 78 wt% SiO_2; Preece *et al.,* 2014). However, differences between the glass chemistry compositions of the White River Ash east and White River Ash north are subtle, and Preece *et al.*, (2014) conclude major element glass chemistry alone cannot consistently discriminate between the White River Ash east and White River Ash north. As such J63 cannot yet be securely correlated to either the White River Ash east or White River Ash north.

Tephra J118

Sample J118 consists of clear, highly vesicular, blocky, and pumiceous shards, forming a pale yellow layer <1mm thick. Glass chemistry is rhyolitic with high Cl values (0.34 - 0.41 wt%; Figure 3). The modeled age range is 4580-3740 cal yr BP, based on the tephra bed's position in the Carlson and Finney (2004) record, who noted J118 at a depth of 138 cm (Figure 2). They attributed it to the Jarvis Creek tephra set.

Glass chemistry from J118 is similar to that of the Hayes tephra set H, particularly layer F2 (Figure 3). The Hayes tephra set H is formed of 7-8 closely spaced ash layers originating from Mt Hayes between ~4200-3700 cal yr BP and includes the Jarvis Creek tephra set (Riehle, 1985; Wallace *et al.,* 2014). Layer F2, also known as Jarvis Ash/unit G (Riehle 1994), is the only Holocene tephra previously found in interior

Alaska, and has an estimated age range of 4205-3910 cal yr BP (Davies *et al.*, 2016). This is within the modelled age range of J118 from this study.

Tephra J127

Sample J127 consists of vesicular, blocky, and pumiceous shards, commonly with mineral inclusions, forming a discrete layer <1mm thick. Glass chemistry has a high and narrow range of SiO_2 (76.32 - 77.20 % wt) and distinctively low K_2O values (0.17 - 0.27 %wt; Figure 3). The modeled age range is 4820-4240 cal yr BP, based on the tephra bed's position in the record of Carlson and Finney (2004), who noted J127 at a depth of 149cm where it is attributed to the Jarvis Creek tephra set (Fig. 2).

The modelled age range for J127 (4820-4240 cal yr BP) predates both the reported age of the Hayes tephra set H, and basal dates from proximal tephra fall deposits on the Hayes River (Reihle, 1994; Wallace *et al*., 2014). Glass chemistry of J127 shows limited overlap with Mt. Hayes reference material (UA 2614 Hayes F2) and a different abundance of major elements, including higher SiO_2 and lower K_2O (Figure 3). Based on whole rock and individual glass shard analyses, Fierstein and Hildreth, (2008) proposed this combination of high SiO_2 and low K_2O is unique to Mt. Augustine and Mt. Kaguyak on the Alaska Peninsula. There are few examples of distal tephra beds linked to either volcano but proximal deposits indicate Mt. Augustine and Mt. Kaguyak have been active within the modelled age range of J127 (Riehle *et al*., 1996). Thus it seems likely that J127 is derived from one of these volcanic centres.

Brooks Range – Ruppert Lake and WBP

RS94 and RC108 (Ruppert Tephra)

The two sediment cores from Ruppert Lake each contain cryptotephra layers (RC108 and RS94) at similar stratigraphic positions (Fig. 5). Shards from both layers consist of cuspate platy shards, and glass chemistry is rhyolitic with low K_2O values with (1.82 - 2.16 % wt). As these cryptotephras are from similar stratigraphic positions and are chemically indistinguishable (Fig. 6), we consider them to represent the same tephra horizon, which we informally name the "Ruppert tephra". The modelled age of the Ruppert tephra is 3230-2930 cal yr BP in RS and 2920-2520 cal yr BP in RC (Fig. 5).

The glass chemistry of the Ruppert tephra is similar to the NDN 230 cryptotephra from Nordan's Bog, Newfoundland (Pyne O'Donnell *et al.*, 2012; Figure 6). However, the reported age range for NDN 230 (2320-2110 cal yr BP) is slightly younger than the modelled age of the Ruppert tephra, and it is unclear whether this difference reflects age model errors or if the tephras were produced during separate eruptions. The NDN 230 tephra was initially linked to Augustine unit G, however, as discussed by Mackay *et al.*, (2016), this correlation is now considered unlikely, and the origin of both tephras remains unclear.

RS126, RC127 and WBP65 (Aniakchak CFE II)

A cryptotephra layer of clear platy shards is found at similar stratigraphic positions in all three Brooks Range cores (RS126, RC127 and WBP 65 of Fig. 5). The rhyolitic glass chemistry is identical for all three layers. The Modelled age ranges are 3670-3200 cal yr BP in RC, 3650-3180 cal yr BP in RS and 4110-3740 cal yr BP in WBP.

Glass chemistry from all three layers is indistinguishable from the higher SiO_2 population of Aniakchak Caldera Forming Event II (CFE II), reference material UA1602 (Fig. 6), and the modelled age ranges from both Ruppert Lake cores are consistent with the ~3600 cal yr BP caldera forming event of Aniakchak. However, the modeled age range for the Aniakchak CFE II tephra in WBP is older (4110-3740 cal yr BP). This offset is possibly an artifact of an erroneously older date obtained from a macrofossil at 63 cm that modifies the modelled sedimentation rate (Fig. 5). Nonetheless, this tephra is likely also the Aniakchak CFE II because of the strong geochemical correlation between the WBP tephra and the Ruppert Lake tephras. The Aniakchak CFE II was amongst the largest eruptions to take place during the Holocene producing an estimated eruptive volume of > 50km^3 (Riehle *et al*., 1987; Neal *et al*., 2001). Volcanic ash layers extend northwards from Aniakchak volcano (Beget *et al.*, 1992; Kaufman *et al*., 2012; Pearce *et al.,* 2016), and cryptotephra associated with the eruption is described in several North Atlantic records (Pyne O'Donnell *et al*., 2012; Jennings *et al*., 2014), as well as in the Mt. Logan ice core (Zdanowicz *et al*., 2014) and Greenland ice cores, where it is dated to 3595±4 cal yr BP (Denton and Pearce, 2008; Coulter *et al.,* 2012).

RS151

RS151 consists of clear platy shards with major element geochemistry indistinguishable from the Aniakchak CFE II tephra (Fig. 6). The cryptotephra is only found in RS, where it forms an independent shard peak dated to 4070-3760 cal yr BP.

Discussion

Interpretation of RS151; a precursor to the Aniakchak CFE II eruption

The RS core contains two cryptotephras 25 cm apart with glass chemistry that correlates closely to the Aniackchak CFE II tephra. However, preservation of RS151 in only one of the studied cores, combined with identical glass chemistry and shard morphology with the Aniakchak CFE II preserved above it, complicates description of the tephra as an independent isochron. The Aniakchak CFE II (RS126) and RS151 occur either side of a section break in the core (at 137 cm). However, sediment geochemistry values differ strongly between samples (supplementary information Table S5, Fig. 2) eliminating any possibility of core overlap and hence repeated sampling. One explanation is that RS151 is the result of the downward movement of shards through soft organic sediments, via density induced displacement or bioturbation. Such post-depositional reworking has been described for discrete visible ash beds (Anderson *et al*., 1984; Beierle and Bond, 2002) and cryptotephra layers (Davies *et al*., 2007). However, the sinking tephra would be expected to produce an evident downward tail of shards that is not observed in RS. In addition, both Ruppert cores contain undisturbed laminations that would be distorted by any bioturbation or slumping, suggesting tephras within Ruppert Lake are preserved *in situ*. Thus, it seems likely RS151 is an independent tephra derived from a pre-caldera eruption of the Aniakchak volcano. Previous studies show that pre-caldera tephras from Aniakchak volcano can share similar glass chemistry to the CFE II (Kaufman *et al*., 2012). Neal *et al.* (2001) acknowledged at least twenty explosive Holocene eruptions prior to the ~3600 cal yr BP caldera event, and it is likely RS151 represents one of these events.

Implications of distal records of Alaska tephra

Discovery of cryptotephra in the Brooks Range and characterisation of beds in the eastern interior shows the potential of tephrochronology for refining stratigraphic and chronological uncertainties across Alaska. In particular, identification of the Aniakchak CFE II tephra in high concentrations, in all three Brooks Range cores shows the tephra to be a regional and precisely dated stratigraphic marker for the mid-late Holocene in northern Alaska. Such well dated horizons are particularly valuable in Alaska, where reworking of old (Holocene) carbon can reduce the accuracy of radiocarbon dating (Abbott and Stafford, 1996).

The geochemical description of the White River Ash and Hayes F2 layer in Jan Lake provide similar correlation opportunities in the eastern interior, and discovery of a new tephra bed linked to an Aleutian arc-Alaska Peninsula source (mostly likely Mt. Augustine or Mt. Kaguyak) may provide a new stratigraphic marker for interior Alaska. Although further work is needed, the potential correlation between the Ruppert tephra in the Brooks Range and the NDN 230 tephra in Newfoundland (Pyne O'Donnell *et al*., 2012) may enable correlation between the two regions and across North America.

Tephra preservation in the Brooks Range

The Brooks Range records contain comparatively few tephras given the relative proximity of study sites to volcanic sources in Kamchatka and the Aleutian Arc-Alaska Peninsula. Eruptions from these centers have produced intercontinental cryptotephra horizons (Coulter *et al*., 2012; Pyne O'Donnell *et al*., 2012; Mackay *et al*., 2016), however, few of these are found in Ruppert Lake or WBP. This likely reflects prevailing atmospheric circulation, with the Brooks Range situated north of the Arctic front for much of the year, and therefore subject to predominately north-easterly winds (Serreze *et al*., 2001). Although the Brooks Range sites contain fewer tephras, low background levels of volcanic shards facilitate identification of cryptotephras that may be obscured in more proximal localities. These horizons are likely to add to the eruption histories of Alaska, and possibly Kamchatka, volcanoes.

The tephrostratigraphies of all three Brooks Range cores differ, despite the proximity of Ruppert Lake to WBP. Notably, the Ruppert tephra (RC108 and RS94) is absent from WBP, while only RS preserves a tephra predating the Aniakchak CFE II. The hydrological isolation of WBP means any preserved tephra must be from primary air fall, whereas Ruppert Lake is fed by two inlets draining a much larger catchment (Figures 1, 4). Catchment size, surface area and inlet presence affect the delivery and distribution of volcanic shards across a basin (Mangerud, 1984; de Fontaine *et al.,* 2007; Pyne O'Donnell, 2011), and It is likely the absence of inlets to WBP, combined with a smaller catchment and surface area, make the lake less effective in entrapping distal tephras where lower volcanic ash concentrations were available.

Conclusions

- Major and minor-element analysis of tephra in the Alaska eastern interior document a White River Ash tephra, the Hayes tephra set H (layer F2) and a new ash layer, likely to be associated with Mt. Augustine or Mt. Kaguyak.

- At least three cryptotephras are present in the Brooks Range, including the ~3600 cal yr BP Aniakchak CFE II tephra and a late Holocene eruption with similar glass chemistry to the NDN 230 tephra preserved in Newfoundland (Pyne O’Donnell *et al.*, 2012). The discovery of cryptotephra well beyond the extent of visible ash layers shows the potential for tephrochronology to refine northern Alaska stratigraphy and chronology.
- A cryptotephra (RS151) chemically identical to the Aniakchak CFE II but preserved stratigraphically below it was most likely deposited by an explosive eruption of the Aniakchak volcano closely pre-dating the ~3600 cal yr BP caldera event.

Acknowledgments

The assistance of Dr. Victoria Smith in the geochemical analyses of tephra at the University of Oxford is greatly appreciated, while Charlotte Clarke kindly helped in the preparation of samples and Mark Dover provided cartographic expertise. An anonymous reviewer, along with Prof. Chris Turney and the Quaternary Research editors, Dr. Jim O’Connor and Prof. Lewis Owen, provided constructive criticisms which improved the manuscript. The support of the Quaternary Research Association in funding initial electron-microprobe analysis at the University of Oxford is also gratefully acknowledged. This work was supported by the NERC Radiocarbon Facility NRCF010001 (allocation numbers 1726.0813, 1847.1014, 1946.1015) and a Natural Science and Engineering Research Council Discovery Grant to DF. This research was funded through a grant from the NERC Artic Program no. NE/K000233/1, the LAC project (Lakes and the Arctic Carbon Cycle).

References cited

Abbott, M. B., Stafford, T. W., 1996. Radiocarbon Geochemistry of Modern and Ancient Arctic Lake Systems, Baffin Island, Canada. Quaternary Research 45, 300 – 311.

Alaska Department of Fish and Game, 2016. Jan Lake Bathymetric Map and Fishing Information. Available at: http://www.adfg.alaska.gov (accessed 22.12.16.).

Anderson, R., Nuhfer, E., Dean, W. E., 1984. Sinking of volcanic ash in uncompacted sediment in Williams Lake, Washington. Science 225, 505 – 508.

Beierle, B., Bond, J., 2002., Density-induced settling of tephra through organic lake sediments. Journal of Paleolimnology 28(4), 433 – 440.

Begét, J., Mason, O., Anderson, P., 1992. Age, extent and climatic significance of the c.3400 BP Aniakchak tephra, western Alaska, USA. The Holocene 2, 51 – 56.

Blaauw, M., Christen, J. A., 2011. Flexible paleoclimate age-depth models using an autoregressive gamma process. Bayesian Analysis 6(3), 457 – 474.

Blockley, S. P. E., Pyne-O'Donnell, S. D. F., Lowe, J.J., Matthews, I.P., Stone, A., Pollard, A.M., Turney, C. S. M., Molyneux. E. G., 2005. A new and less destructive laboratory procedure for the physical separation of distal glass tephra shards from sediments. Quaternary Science Reviews 24(16), 1952 – 1960.

Brubaker, L.B., Garfinkel, H.L., Edwards, M.E., 1983. A Late Wisconsin and Holocene Vegetation History from the Central Brooks Range: Implications for Alaskan Palaeoecology. Quaternary Research 20, 194 – 214.

Brubaker, L.B., Anderson, P.A., Edwards, M.E., Lozhkin, A.V., 2005. Beringia as a Glacial Refugium for Boreal Trees and Shrubs: New Perspectives from Mapped Pollen Data. Journal of Biogeography 32, 833 – 848.

Carlson, L. J., Finney, B. P., 2004. A 13000-year history of vegetation and environmental change at Jan Lake, east-central Alaska. The Holocene 14, 818 – 827.

Cooper, A., Turney, C., Hughen, K.A., Brook, B.W., McDonald, H.G., Bradshaw, C.J.A., 2015. Abrupt warming events drove Late Pleistocene Holarctic megafaunal turnover. Science 349, 602 – 606.

Coulter, S.E., Pilcher, J.R., Plunkett, G., Baillie, M., Hall, V.A., Steffensen, J.P., Vinther, B.M., Clausen, H.B., Johnsen, S.J., 2012. Holocene tephras highlight complexity of volcanic signals in Greenland ice cores. Journal of Geophysical Research: Atmospheres 117(D21).

Cushing, E. J., Wright, H. E., 1965. Hand-operated piston corers for lake sediments. Ecology 46, 380 – 384.

Davies, S. M., Elmquist, M., Bergman, J., Wohlfarth, B., Hammarlund, D., 2007. Cryptotephra sedimentation processes within two lacustrine sequences from west central Sweden. The Holocene 17(3), 319 – 330.

Davies, L.J., Jensen, B.J.L., Froese, D.G., Wallace, K.L., 2016. Late Pleistocene and Holocene tephrostratigraphy of interior Alaska and Yukon: Key beds and chronologies over the past 30,000 years. Quaternary Science Reviews 146, 28 – 53.

Denton J.S., Pearce N.J.G., 2008. Comment on ‘A synchronized dating of three Greenland ice cores through the Holocene’ by B.M. Vinther *et al*.: no Minoan tephra in the 1642 B.C. layer of the GRIP ice core. Journal of Geophysical Research 113: D04303.

de Fontaine, C. S., Kaufman, D. S., Anderson, R. S., Werner, A., Waythomas, C. F., Brown, T. A., 2007. Late Quaternary distal tephra-fall deposits in lacustrine sediments, Kenai Peninsula, Alaska. Quaternary Research 68(1), 64 – 78.

Edwards, M.E., Anderson, P.M., Garfinkel, H.L., Brubaker, L.B., 1985. Late-Wisconsin and Holocene vegetation history of the upper Koyukuk region, central Brooks Range, Alaska. Canadian Journal of Botany 63, 6l6 – 626.

Fierstein, J., Hildreth, W., 2008. Kaguyak dome field and its Holocene caldera, Alaska Peninsula. Journal of Volcanology and Geothermal Research 177(2), 340 – 366.

Guthrie, R.D., 2006. New carbon dates link climatic change with human colonization and Pleistocene extinctions. Nature 441, 207 – 209.

Higuera, P.E., Brubaker, L.B., Anderson, P.M., Hu, F.S., Brown, T.A., 2009. Vegetation mediated the impacts of postglacial climate change on fire regimes in the south-central Brooks Range, Alaska. Ecological Monographs 79(2), 201 – 219.

Jennings, A., Thordarson, T., Zalzal, K., Stoner, J., Hayward, C., Geirsdóttir, Á., Miller, G., 2014. Holocene tephra from Iceland and Alaska in SE Greenland shelf sediments. Geological Society London, Special Publications.

Jensen, B.J.L., Froese, D.G., Preece, S.J., Westgate, J.A., Stachel, T., 2008. An extensive middle to late Pleistocene tephrochronologic record from east-central Alaska. Quaternary Science Reviews 27, 411 – 427.

Jensen, B. J., Pyne-O'Donnell, S., Plunkett, G., Froese, D. G., Hughes, P. D., Sigl, M., McConnell, J.R., Amesbury, M.J., Blackwell, P.G., van den Bogaard, C., Buck, C.E., Charman, D.J., Clague, J.J., Hall, V.A., Koch, J., Mackay, H., Mallon, G., McColl, L., Pilcher, J. R., 2014. Transatlantic distribution of the Alaskan White River Ash. Geology 42(10), 875 – 878.

Kaufman, D. S., Jensen, B. J., Reyes, A. V., Schiff, C. J., Froese, D. G., Pearce, N. J., (2012). Late Quaternary tephrostratigraphy, Ahklun Mountains, SW Alaska. Journal of Quaternary Science 27 (4), 344 – 359.

Kuehn, S.C., Froese, D.G., Shane, P.A.R., Participants, I.I., 2011. The INTAV intercomparison of electron-beam microanalysis of glass by tephrochronology laboratories: results and recommendations. Quaternary International 246(1), 19 – 47.

Lerbekmo, J. F., 2008. The White river ash: largest Holocene Plinian tephra. Canadian Journal of Earth Sciences 45(6), 693 – 700.

Lowe, D.J., 2011. Tephrochronology and its application: A review. Quaternary Geochronology 6, 107 – 153.

Mackay, H., Hughes, P.D.M., Jensen, B.J.L., Langdon, P.G., Pyne-O’Donnell, S., Plunkett, G., Froese, D.G., Coulter, S., 2015. The foundations of a late Holocene tephrostratigraphic framework for eastern North America. Quaternary Science Reviews 132, 101 – 113.

Mangerud, J., Lie, S. E., Furnes, H., Kristiansen, I. L., Lømo, L. 1984. A Younger Dryas ash bed in western Norway, and its possible correlations with tephra in cores from the Norwegian Sea and the North Atlantic. Quaternary Research 21, 85 – 104.

Miller, T. P., Smith, R. L., 1987. Late Quaternary caldera-forming eruptions in the eastern Aleutian arc, Alaska. Geology 15(5), 434 – 438.

Neal, C. A., McGimsey, R. G., Miller, T. P., Riehle, J. R., Waythomas, C. F., 2001. Preliminary volcano-hazard assessment for Aniakchak Volcano, Alaska. US Geological Survey, No. 00 – 519.

Oswald, W.W., Gavin, D.G., Anderson, P.M., Brubaker, L.B., Hu, F-S., 2012. A 14,500-year record of landscape change from Okpilak Lake, northeastern Brooks Range, northern Alaska. Journal of Paleolimnology 48, 101 – 113.

Payne, R.J., Blackford, J.J., 2004. Distal micro-tephra deposits in southeast Alaskan peatlands. In: D.S. Emond., L.L. Lewis. (eds.), Yukon Exploration and Geology 2003, Yukon Geological Survey, 191 – 197.

Payne, R., Blackford, J., 2008. Extending the late Holocene tephrochronology of the Kenai Peninsula, Alaska. Arctic 61, 243 – 254.

Payne, R., Blackford, J., van der Plicht, J., 2008. Using cryptotephras to extend regional tephrochronologies: an example from southeast Alaska and implications for hazard assessment. Quaternary Research 69(1), 42 – 55.

Pearce, C., Varhelyi, A., Wastegård, S., Muschitiello, F., Barrientos, N., O'Regan, M., Cronin, T., Gemery, L., Semiletov, I., Backman, J., Jakobsson, M., 2016. The 3.6 ka Aniakchak tephra in the Arctic Ocean: a constraint on the Holocene radiocarbon reservoir age in the Chukchi Sea, Climate of the Past Discussions doi:10.5194/cp-2016-112, in review.

Preece, S. J., McGimsey, R. G., Westgate, J. A., Pearce, N. J. G., Hart, W. K., Perkins, W. T., 2014. Chemical complexity and source of the White River Ash, Alaska and Yukon. Geosphere, GES00953 – 1.

Pyne O'Donnell, S.D.F., 2011. The taphonomy of Last Glacial–Interglacial Transition (LGIT) distal volcanic ash in small Scottish lakes. Boreas 40(1), 131 – 145.

Pyne O'Donnell, S.D.F., Hughes, P.D.M., Froese, D.G., Jensen, B.J.L., Kuehn, S.C., Mallon, G., Amesbury, M.J., Charman, D.J., Daley, T.J., Loader, N.J., Mauquoy, D., Street-Perrott, F.A., Woodman-Ralph, J., 2012. High-precision ultra-distal Holocene tephrochronology in North America. Quaternary Science Reviews 52, 6 – 11.

Reimer, P., Bard, E., Bayliss, A., Beck, J., Blackwell, P., Bronk Ramsey, C., Buck, C., Cheng, H., Edwards, R., Friedrich, M., 2013. IntCal13 and Marine13 radiocarbon age calibration curves 0-50,000 years cal BP. Radiocarbon 55, 1869 – 1887.

Riehle, J. R., 1985. A reconnaissance of the major Holocene tephra deposits in the upper Cook Inlet region, Alaska. Journal of Volcanology and Geothermal Research 26, 37 – 74.

Riehle, J. R., Meyer, C. E., Ager, T. A., Kaufman, D. S., Ackerman, R. E., 1987. The Aniakchak tephra deposit, a late Holocene marker horizon in western Alaska. US Geological Survey Circular 998, 19 –22.

Riehle, J. R., 1994. Heterogeneity, correlatives, and proposed stratigraphic nomenclature of Hayes tephra set H, Alaska. Quaternary Research 41(3), 285 – 288.

Riehle, J.R., Waitt, R.B., Meyer, C.E., Calk, L.C., 1996. Age of formation of Kaguyak caldera, eastern Aleutian arc, Alaska, estimated by tephrochronology. Geologic Studies in Alaska by the US Geological Survey.

Serreze, M.C., Lynch, A.H., Clark, M.P., 2001. The Arctic frontal zone as seen in the NCEP-NCAR reanalysis. Journal of Climate 14(7), 1550 – 1567.

Turney, C. S.M., 1998. Extraction of rhyolitic component of Vedde microtephra from minerogenic lake sediments. Journal of Paleolimnology 19(2), 199 – 206.

Wallace, K., Coombs, M. L., Hayden, L. A., Waythomas, C. F., 2014. Significance of a near-source tephra-stratigraphic sequence to the eruptive history of Hayes Volcano, south-central Alaska. US Geological Survey, 2014 – 5133.

Wright, H.E., Mann, D.H., Glaser, P.H., 1984. Piston corers for peat and lake sediments. Ecology 65, 657 – 59.

Zander, P. D., Kaufman, D. S., Kuehn, S. C., Wallace, K. L., Anderson, R. S., 2013. Early and late Holocene glacial fluctuations and tephrostratigraphy, Cabin Lake, Alaska. Journal of Quaternary Science 28(8), 761 – 771.

Zdanowicz, C. M., Zielinski, G. A., Germani, M. S., (1999). Mount Mazama eruption: Calendrical age verified and atmospheric impact assessed. Geology 27(7), 621 – 624.

Zdanowicz, C., Fisher, D., Bourgeois, J., Demuth, M., Zheng, J., Mayewski, P.A., Kreutz, K., Osterberg, E., Yalcin, K., Wake, C., Steig, E.J., Froese, D.G., Goto- Azuma, K., 2014. Ice cores from the St. Elias Mountains, Yukon, Canada: their significance for climate, atmospheric composition and volcanism in the north Pacific region. Arctic 67, 35 – 57.

List of figures (including captions)

Figure 1: (a) Map of Alaska and the location of study sites shown with volcanic sources. The approximate visible limits of the key tephra beds are re-drawn from Davies *et al.,* (2016). (b) Surrounding topography and lake catchments (illustrated by dashed line) of Brooks Range sites. (c) Surrounding topography of Jan Lake. Colour version available online.

Figure 2: Range finder shard counts and age models produced for the Jan Lake core (this study), and stratigraphy and updated age model from Carlson and Finney, (2004). Tephras correlated between sequences based on stratigraphic position are denoted by dotted lines.

Figure 3: Bivariate plots of major and minor element glass chemistry from Jan Lake tephras, plotted against White River Ash east (WRAe) (Jensen *et al*., 2014), White River Ash north (WRAn) and the Hayes F2 tephra (Davies *et al*., 2016). Colour version available online.

Figure 4: Lake morphology, including bathymetry and coring locations for Ruppert Lake (a), WBP (b) and Jan Lake (c). Depth isopleths are shown in centimeters and were derived using measurements taken with a depth sounder, with the exception of Jan Lake were bathymetry values are taken from those presented by the Alaska Department of Fish and Game (www.adfg.alaska.gov, December 2016).

Figure 5: Range finder shard counts and age models produced for Brooks Range cores. Sections of RC that were unlikely to contain tephra based on results from RS and WBP were not counted as all available material was consumed for use in other analyses as part of the Lakes and the Arctic Carbon Cycle project (NERC ref NE/K000233/1).

Figure 6: Bivariate plots of major and minor element glass chemistry from the Brooks Range tephras, plotted against Aniakchak CFE II reference material (UA 1602) run concurrently during analyses, and the NDN 230 tephra from Nordan's Bog, Newfoundland (Pyne O'Donnell *et al*., 2012) (Cl values were not available for NDN 230). Colour version available online.

Figure 1 (Supplementary information, Table S5): Bivariate plots of major and minor element glass chemistry from Jan Lake and Brooks Range tephras, probed at the University of Oxford and the University of Alberta.

Figure 2 (Supplementary information, Table S5): Titanium values used in the correlation of clay bands between RS and RC.

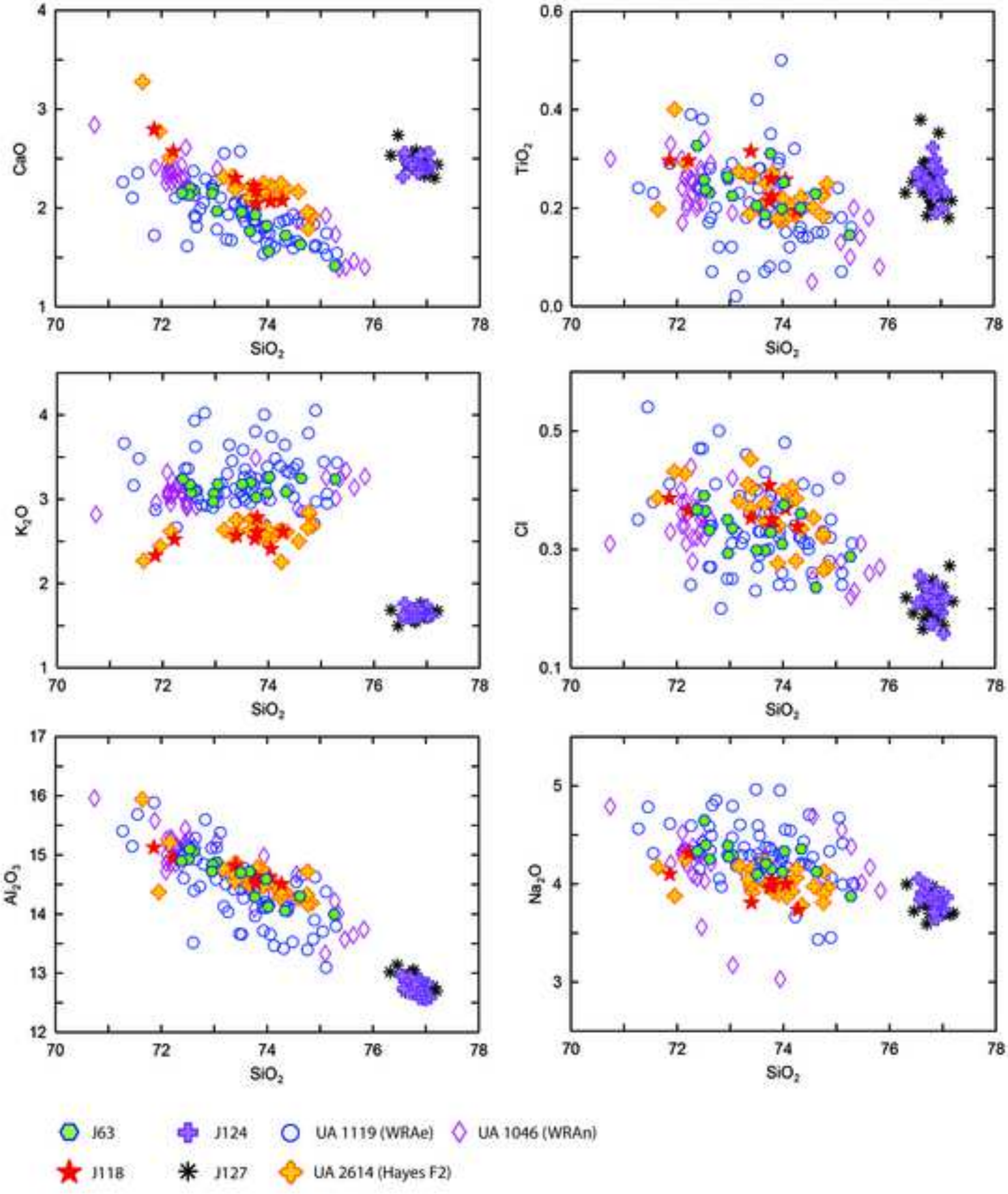

CaO
SiO2
TiO2
K2O
Cl
Al2O3
Na2O
J63
J124
UA 1119 (WRAe)
UA 1046 (WRAn)
J118
J127
UA 2614 (Hayes F2)

Figure

Click here to download Figure Figure 3 (greyscale).tif

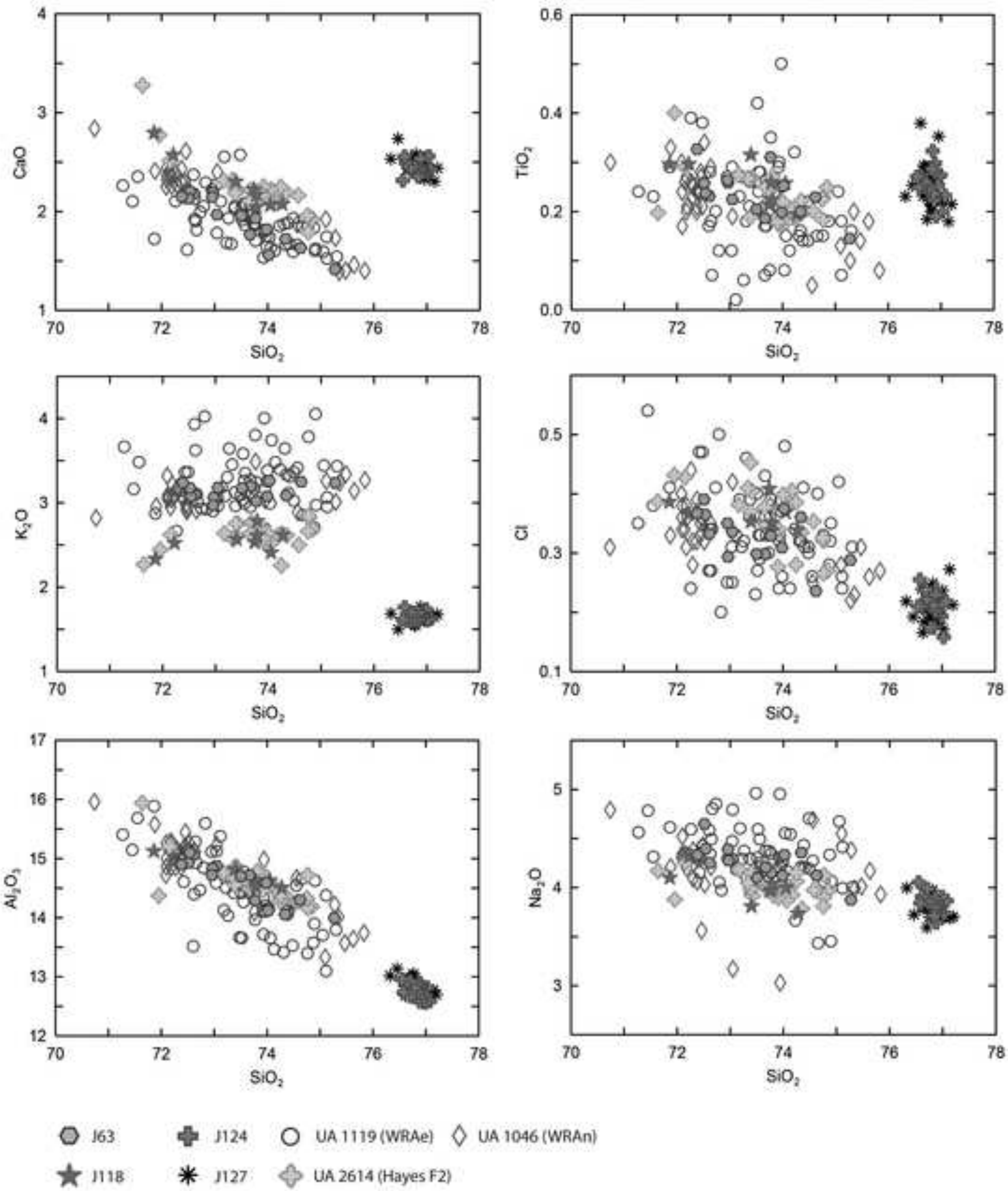

Figure

Click here to download Figure Figure 6 (colour).tif

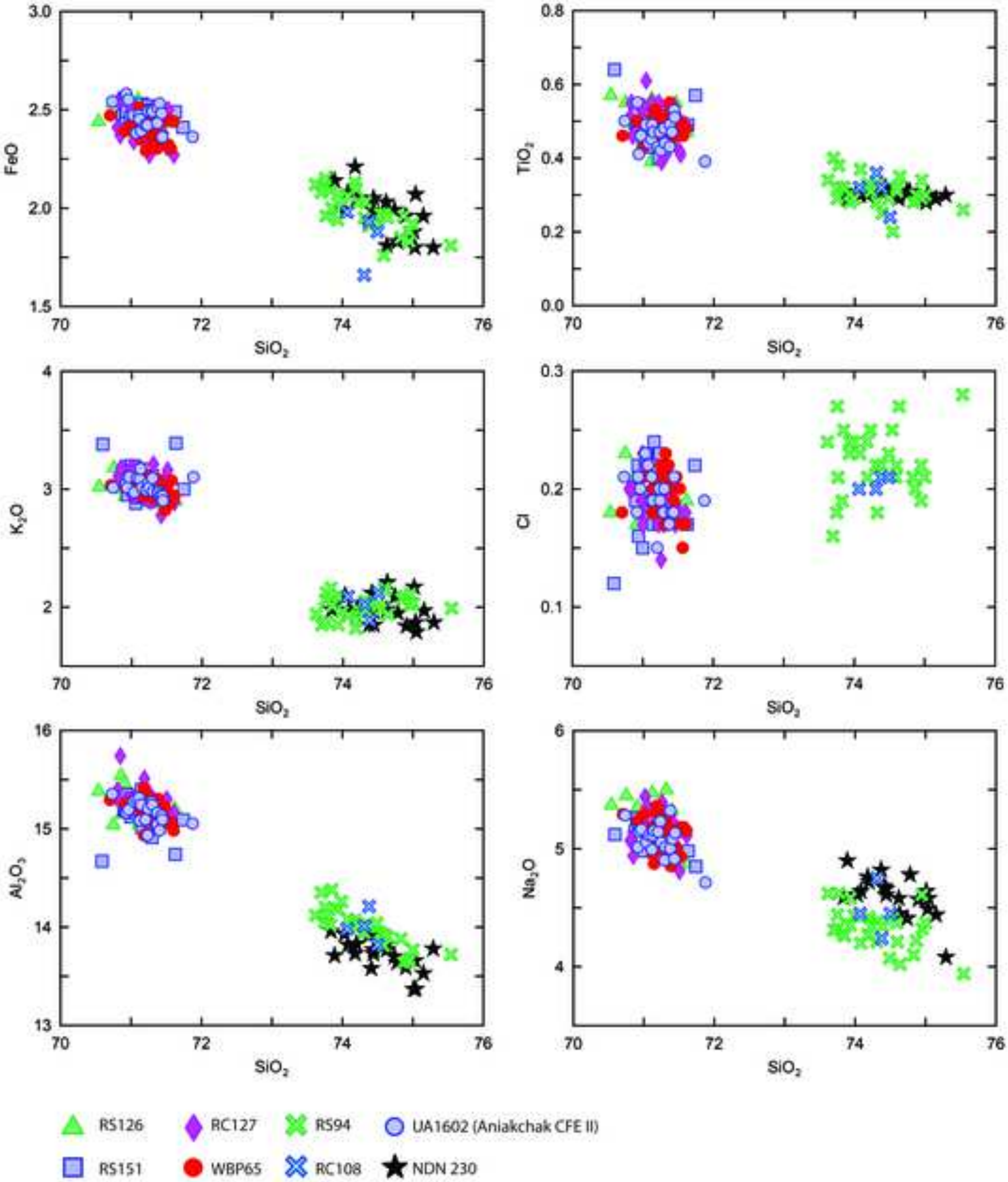

Figure

Click here to download Figure Figure 6 (greyscale).tif

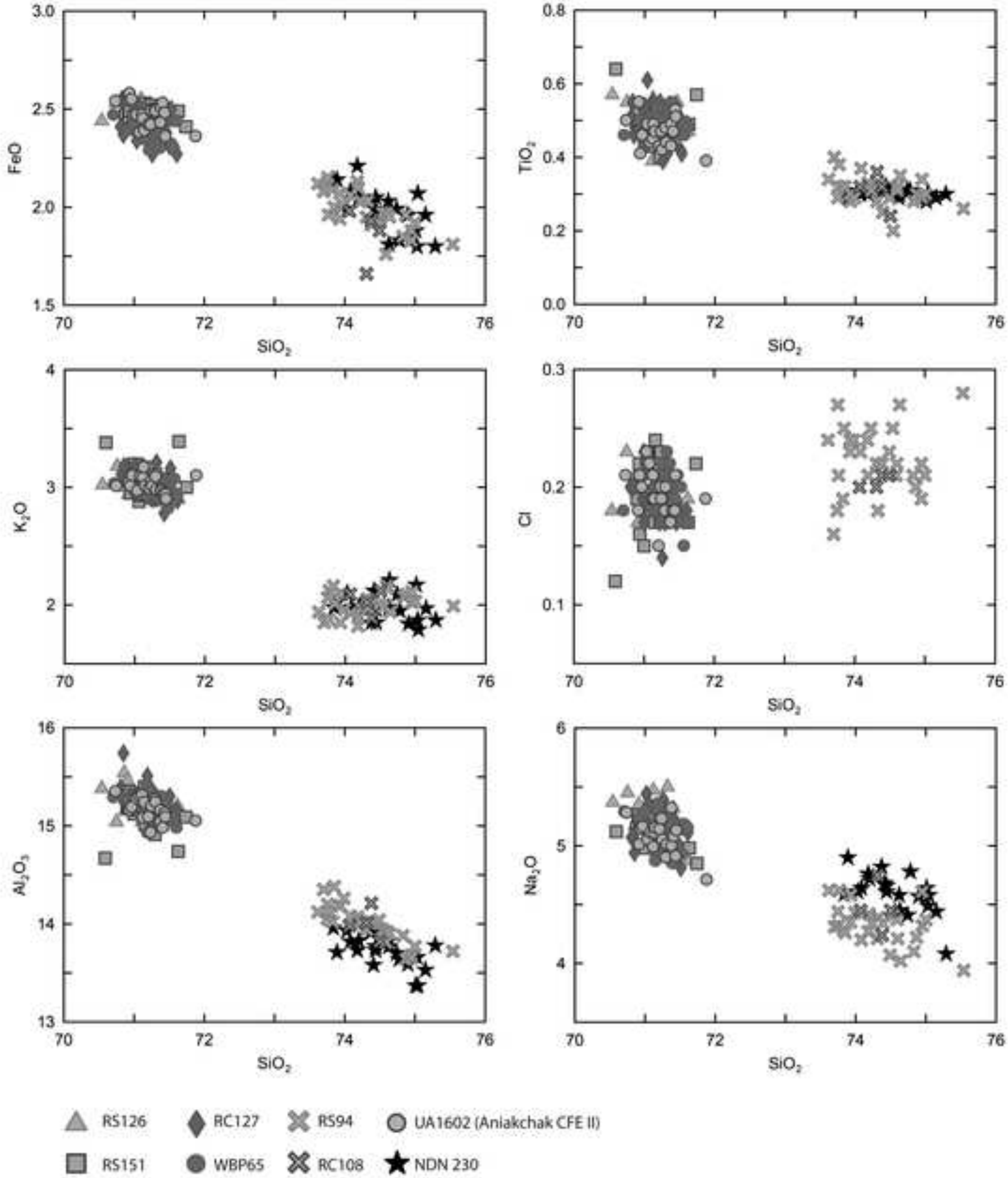

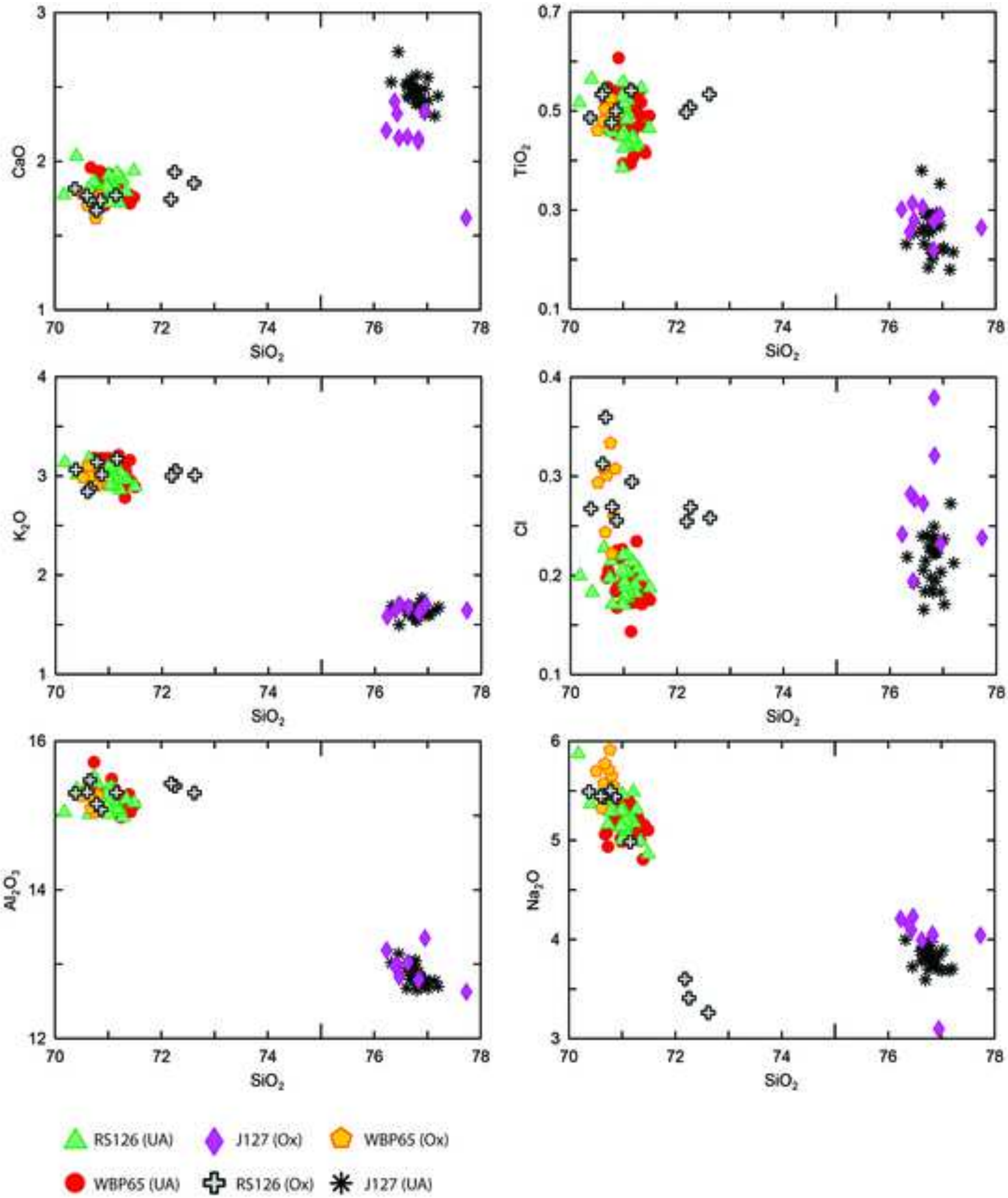

CaO
SiO2
TiO2
SiO2
K2O
SiO2
Cl
SiO2
Al2O3
SiO2
Na2O
SiO2
RS126 (UA)
J127 (Ox)
WBP65 (Ox)
WBP65 (UA)
RS126 (Ox)
J127 (UA)

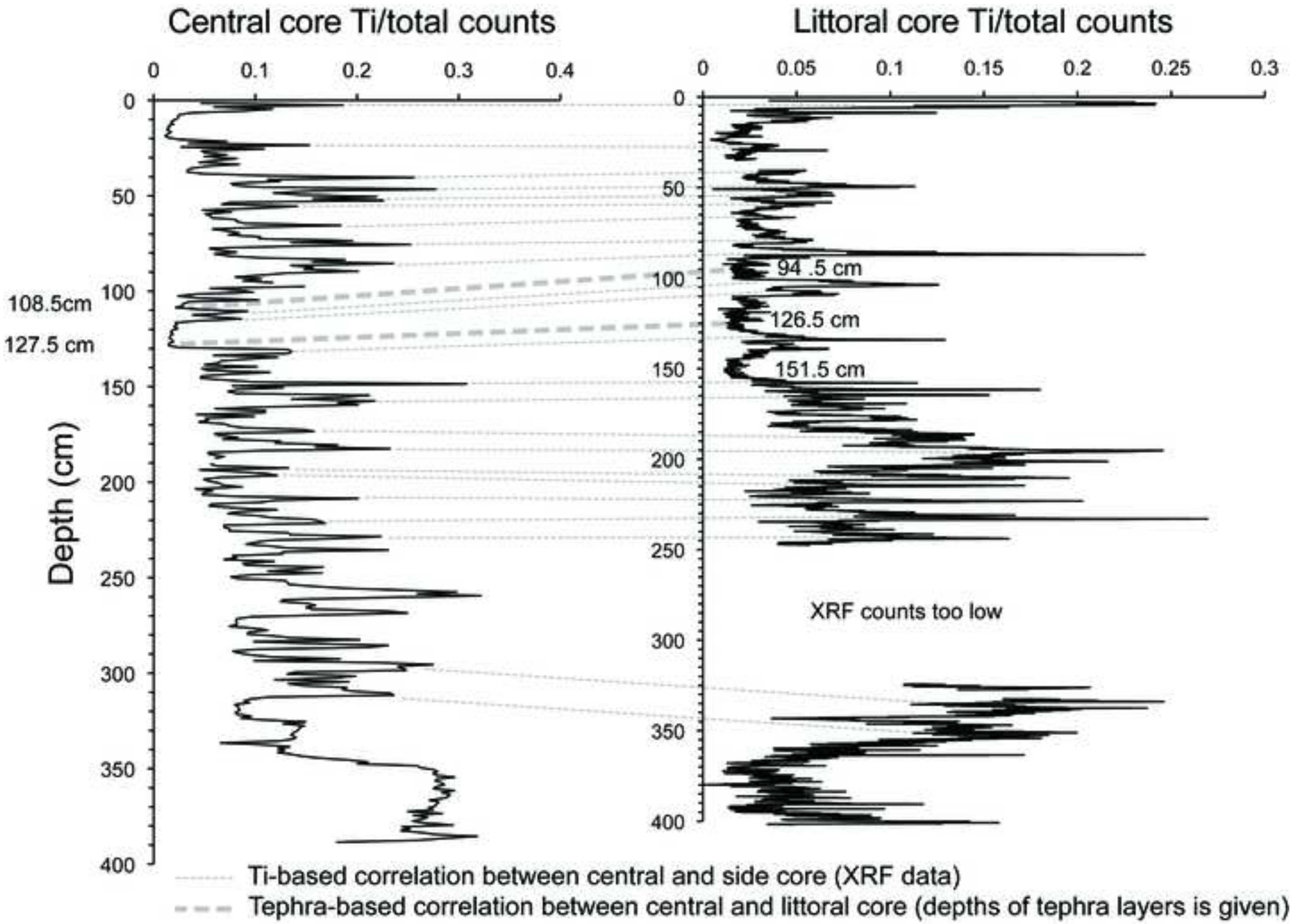
Central core Ti/total counts
Littoral core Ti/total counts
0 0.1 0.2 0.3 0.4
0 0.05 0.1 0.15 0.2 0.25 0.3
Depth (cm)
0 50 100 150 200 250 300 350 400
108.5cm
127.5 cm
94 .5 cm
126.5 cm
151.5 cm
XRF counts too low
Ti-based correlation between central and side core (XRF data)
Tephra-based correlation between central and littoral core (depths of tephra layers is given)

Table S1: Individual EPMA glass shard analyses, included in this study.
Includes data reported in Pyne O'Donnell et al, (2012); Jensen et al, (2014); Davies et al, (2016)
Analytical conditions (Alberta): 10 micron beam, 15 KeV and 6 nA current
Data normalised to 100%. STDEV = standard deviation.

Tephra	Sample	SiO_2	TiO2	Al_2O_3	FeO_T	MnO	MgO	CaO	Na_2O	K_2O	Cl	Total	H2O Diff	n	Comments/ Correlations
J63															
	UA 2553_30	72.38	0.33	14.90	1.85	0.00	0.46	2.15	4.33	3.24	0.37	100	2.41		
	UA 2553_11	72.51	0.26	14.92	1.56	0.04	0.36	2.13	4.65	3.18	0.39	100	5.46		
	UA 2553_22	72.54	0.24	15.10	1.69	0.03	0.37	2.20	4.39	3.08	0.36	100	2.37		
	UA 2553_7	72.62	0.23	15.06	1.74	0.08	0.42	2.18	4.25	3.09	0.33	100	1.80		
	UA 2553_21	72.96	0.26	14.72	1.73	0.10	0.37	2.15	4.39	2.97	0.35	100	2.06		
	UA 2553_13	72.97	0.26	14.83	1.64	0.05	0.43	2.19	4.28	3.06	0.29	100	2.84		
	UA 2553_8	73.05	0.22	14.87	1.68	0.04	0.36	1.97	4.29	3.18	0.34	100	1.66		
	UA 2553_2	73.50	0.20	14.70	1.62	0.04	0.39	1.96	4.10	3.18	0.30	100	1.88		
	UA 2553_28	73.67	0.19	14.71	1.57	0.04	0.36	1.77	4.20	3.20	0.30	100	1.88		
	UA 2553_32	73.77	0.31	14.29	1.76	0.08	0.35	1.93	4.15	3.02	0.33	100	2.65		
	UA 2553_34	73.98	0.20	14.59	1.51	0.08	0.31	1.82	4.12	3.08	0.31	100	2.00		
	UA 2553_19	74.02	0.25	14.12	1.66	0.03	0.38	1.56	4.33	3.26	0.38	100	1.20		
	UA 2553_17	74.34	0.20	14.06	1.46	0.07	0.35	1.72	4.36	3.09	0.36	100	1.60		
	UA 2553_6	74.62	0.23	14.30	1.32	0.03	0.26	1.63	4.12	3.25	0.24	100	1.68		
	UA 2553_14	75.27	0.15	14.00	1.41	0.05	0.31	1.41	3.87	3.24	0.29	100	2.10	15	
	Mean	73.48	0.24	14.61	1.61	0.05	0.37	1.92	4.26	3.14	0.33	100	2.24		White River Ash correlative
	STDEV	0.86	0.05	0.37	0.14	0.03	0.05	0.26	0.18	0.09	0.04	0	0.99		
J118															
	UA 2554_23	74.28	0.19	14.51	1.60	0.14	0.52	2.08	3.74	2.62	0.34	100	3.44		
	UA 2554_10	73.79	0.26	14.53	1.66	0.13	0.48	2.17	4.04	2.61	0.34	100	1.39		
	UA 2554_24	73.79	0.22	14.61	1.64	0.07	0.51	2.04	3.98	2.78	0.35	100	2.37		

	UA 2554_17	74.05	0.26	14.63	1.67	0.05	0.49	2.06	4.00	2.41	0.37	100	3.19		
	UA 2554_31	73.74	0.21	14.63	1.70	0.04	0.54	2.22	3.96	2.53	0.41	100	2.11		
	UA 2554_4	73.40	0.32	14.82	1.79	0.08	0.57	2.30	3.81	2.57	0.35	100	2.39		
	UA 2554_13	72.22	0.30	14.94	1.97	0.07	0.72	2.57	4.31	2.52	0.37	100	2.39		
	UA 2554_26	71.86	0.30	15.12	2.18	0.13	0.80	2.80	4.10	2.33	0.39	100	2.43		
	Mean	73.39	0.26	14.72	1.78	0.09	0.58	2.28	3.99	2.55	0.36	100	2.46	8	
	STDEV	0.88	0.04	0.22	0.20	0.04	0.12	0.27	0.18	0.14	0.02	0	0.63		Hayes F2 correlative
J124															
	UA 2555_3	76.55	0.27	12.96	1.59	0.07	0.37	2.31	4.05	1.62	0.21	100	3.60		
	UA 2555_13	76.58	0.25	12.74	1.64	0.00	0.38	2.56	3.84	1.76	0.26	100	1.81		
	UA 2555_15	76.61	0.27	12.86	1.59	0.06	0.40	2.49	3.91	1.60	0.21	100	2.29		
	UA 2555_23	76.70	0.26	12.92	1.57	0.06	0.36	2.44	3.86	1.60	0.24	100	2.12		
	UA 2555_29	76.71	0.26	12.67	1.52	0.13	0.39	2.42	3.99	1.69	0.22	100	2.81		
	UA 2555_25	76.78	0.25	12.81	1.65	0.02	0.40	2.45	3.86	1.60	0.17	100	1.86		
	UA 2555_26	76.84	0.29	12.86	1.60	0.08	0.40	2.35	3.71	1.69	0.17	100	1.65		
	UA 2555_28	76.84	0.32	12.74	1.59	0.07	0.39	2.42	3.80	1.62	0.21	100	1.55		
	UA 2555_31	76.86	0.24	12.66	1.61	0.08	0.39	2.38	3.89	1.68	0.21	100	1.21		
	UA 2555_4	76.87	0.22	12.75	1.67	0.06	0.36	2.38	3.78	1.70	0.20	100	1.91		
	UA 2555_10	76.88	0.30	12.89	1.49	0.07	0.39	2.43	3.64	1.67	0.23	100	2.48		
	UA 2555_30	76.88	0.28	12.58	1.54	0.07	0.43	2.53	3.81	1.63	0.24	100	2.40		
	UA 2555_5	76.89	0.23	12.78	1.54	0.08	0.39	2.41	3.78	1.67	0.23	100	2.36		
	UA 2555_18	76.91	0.19	12.84	1.56	0.02	0.38	2.41	3.84	1.65	0.20	100	1.71		
	UA 2555_21	76.94	0.25	12.70	1.65	0.05	0.39	2.41	3.76	1.64	0.20	100	3.09		
	UA 2555_34	76.99	0.27	12.56	1.46	0.10	0.39	2.40	3.90	1.74	0.19	100	2.05		
	UA 2555_33	77.03	0.20	12.81	1.49	0.02	0.37	2.56	3.74	1.61	0.16	100	3.18		
	UA 2555_24	77.08	0.23	12.59	1.55	0.03	0.39	2.42	3.86	1.64	0.22	100	2.45		
	Mean	76.83	0.26	12.76	1.57	0.06	0.39	2.43	3.83	1.66	0.21	100	2.25	18	
	STDEV	0.15	0.03	0.12	0.06	0.03	0.02	0.07	0.10	0.05	0.02	0	0.62		Reworked glass from J127

J127

UA 2556_16	76.32	0.23	13.02	1.56	0.07	0.37	2.53	4.00	1.69	0.22	100	1.68
UA 2556_31	76.46	0.25	13.14	1.58	0.05	0.37	2.74	3.72	1.50	0.19	100	0.77
UA 2556_13	76.61	0.38	12.68	1.50	0.08	0.41	2.52	3.88	1.70	0.24	100	2.41
UA 2556_27	76.63	0.26	12.95	1.60	0.06	0.40	2.51	3.79	1.60	0.21	100	0.93
UA 2556_35	76.64	0.26	12.94	1.61	0.06	0.36	2.44	3.89	1.63	0.17	100	1.31
UA 2556_25	76.66	0.23	12.90	1.59	0.06	0.42	2.43	3.90	1.63	0.18	100	2.18
UA 2556_2	76.67	0.29	12.80	1.57	0.10	0.39	2.52	3.80	1.65	0.22	100	1.46
UA 2556_21	76.70	0.29	12.97	1.58	0.02	0.39	2.55	3.59	1.65	0.24	100	1.96
UA 2556_1	76.74	0.18	12.82	1.49	0.08	0.40	2.50	3.94	1.63	0.23	100	3.34
UA 2556_5	76.75	0.25	13.01	1.52	0.07	0.36	2.45	3.70	1.66	0.23	100	2.78
UA 2556_26	76.77	0.22	13.05	1.51	0.05	0.37	2.45	3.83	1.56	0.20	100	2.34
UA 2556_32	76.78	0.27	12.93	1.56	0.10	0.36	2.39	3.89	1.54	0.19	100	2.33
UA 2556_15	76.80	0.29	12.65	1.54	0.08	0.42	2.58	3.82	1.58	0.24	100	1.14
UA 2556_8	76.81	0.26	12.88	1.53	0.03	0.36	2.44	3.81	1.65	0.22	100	1.25
UA 2556_10	76.81	0.20	12.75	1.56	0.04	0.35	2.49	3.97	1.65	0.18	100	1.03
UA 2556_18	76.83	0.21	12.90	1.63	0.00	0.38	2.40	3.76	1.67	0.24	100	1.42
UA 2556_22	76.83	0.21	12.74	1.55	0.09	0.36	2.48	3.87	1.63	0.25	100	1.69
UA 2556_23	76.83	0.29	12.72	1.66	0.06	0.39	2.42	3.78	1.63	0.22	100	0.99
UA 2556_9	76.85	0.27	12.80	1.57	0.05	0.39	2.39	3.74	1.72	0.22	100	1.61
UA 2556_11	76.86	0.27	12.79	1.61	0.06	0.39	2.43	3.77	1.63	0.19	100	1.06
UA 2556_3	76.89	0.29	12.70	1.55	0.06	0.38	2.40	3.74	1.76	0.22	100	0.98
UA 2556_33	76.96	0.35	12.76	1.56	0.01	0.39	2.49	3.70	1.61	0.18	100	1.93
UA 2556_12	76.96	0.27	12.80	1.54	0.11	0.36	2.33	3.83	1.60	0.20	100	1.19
UA 2556_14	77.01	0.22	12.68	1.54	0.05	0.39	2.56	3.69	1.62	0.24	100	2.17
UA 2556_6	77.03	0.22	12.75	1.52	0.06	0.35	2.41	3.89	1.60	0.17	100	1.49
UA 2556_34	77.14	0.18	12.77	1.53	0.08	0.38	2.31	3.69	1.65	0.27	100	0.80
UA 2556_30	77.20	0.21	12.70	1.50	0.01	0.35	2.44	3.70	1.67	0.21	100	3.03
Mean	76.80	0.25	12.84	1.56	0.06	0.38	2.47	3.80	1.63	0.21	100	1.68

27

	STDEV	0.19	0.05	0.13	0.04	0.03	0.02	0.09	0.10	0.05	0.03	0	0.70	Possible Mt. Augustine/ Mt. Kuygak correlative
RS94														
	UA 2557_35	73.53	0.34	14.10	2.12	0.10	0.53	2.49	4.61	1.93	0.24	100	2.52	
	UA 2557_1	73.59	0.40	14.32	2.08	0.08	0.53	2.71	4.31	1.84	0.16	100	1.22	
	UA 2557_16	73.65	0.32	14.18	2.15	0.09	0.47	2.68	4.32	1.88	0.26	100	1.16	
	UA 2557_24	73.65	0.29	14.03	2.11	0.11	0.60	2.53	4.44	2.06	0.18	100	0.86	
	UA 2557_6	73.67	0.38	14.12	1.96	0.07	0.46	2.40	4.62	2.12	0.21	100	0.70	
	UA 2557_23	73.73	0.32	14.00	2.09	0.16	0.52	2.57	4.28	2.16	0.19	100	1.95	
	UA 2557_17	73.76	0.32	14.36	2.00	0.11	0.49	2.44	4.26	2.01	0.25	100	2.32	
	UA 2557_10	73.83	0.30	14.17	1.94	0.12	0.44	2.53	4.35	2.08	0.24	100	0.93	
	UA 2557_22	73.84	0.28	14.16	2.06	0.09	0.51	2.40	4.57	1.85	0.23	100	2.62	
	UA 2557_12	73.89	0.29	14.24	2.01	0.07	0.50	2.37	4.43	1.96	0.24	100	1.79	
	UA 2557_8	73.98	0.37	14.06	2.06	0.14	0.45	2.59	4.20	1.93	0.23	100	1.98	
	UA 2557_2	74.08	0.33	14.05	2.13	0.09	0.48	2.51	4.26	1.82	0.24	100	1.97	
	UA 2557_14	74.09	0.32	13.97	2.09	0.09	0.41	2.51	4.42	1.89	0.21	100	0.83	
	UA 2557_31	74.13	0.31	14.01	2.03	0.09	0.42	2.46	4.33	1.97	0.25	100	3.77	
	UA 2557_9	74.21	0.28	13.92	1.95	0.09	0.48	2.60	4.20	2.05	0.22	100	0.89	
	UA 2557_25	74.24	0.33	14.00	2.03	0.13	0.48	2.25	4.39	1.97	0.18	100	1.65	
	UA 2557_7	74.29	0.25	13.99	1.91	0.09	0.43	2.44	4.33	2.04	0.22	100	2.21	
	UA 2557_5	74.39	0.29	14.02	1.92	0.11	0.42	2.55	4.06	2.01	0.23	100	1.53	
	UA 2557_32	74.45	0.20	13.92	1.97	0.10	0.40	2.32	4.40	1.98	0.25	100	2.28	
	UA 2557_28	74.50	0.32	13.80	1.76	0.11	0.43	2.36	4.36	2.15	0.21	100	1.82	
	UA 2557_21	74.52	0.31	13.90	1.97	0.09	0.42	2.24	4.21	2.14	0.22	100	2.20	
	UA 2557_4	74.54	0.35	13.89	1.95	0.07	0.46	2.53	4.02	1.94	0.27	100	0.87	
	UA 2557_33	74.69	0.26	13.82	1.94	0.08	0.45	2.32	4.37	1.82	0.25	100	4.02	
	UA 2557_13	74.73	0.27	13.86	1.84	0.15	0.40	2.37	4.10	2.07	0.21	100	1.15	
	UA 2557_30	74.78	0.30	13.62	1.95	0.13	0.44	2.27	4.22	2.09	0.20	100	1.86	
	UA 2557_27	74.86	0.34	13.66	1.87	0.04	0.40	2.21	4.32	2.10	0.19	100	1.61	

	UA 2557_26	74.87	0.29	13.64	1.82	0.10	0.39	2.05	4.60	2.02	0.22	100	2.63		
	UA 2557_29	74.92	0.30	13.75	1.92	0.06	0.36	2.09	4.36	2.03	0.21	100	2.09		
	UA 2557_18	75.45	0.26	13.71	1.81	0.11	0.35	2.11	3.93	1.99	0.28	100	2.87		
	Mean	74.24	0.31	13.98	1.98	0.10	0.45	2.41	4.32	2.00	0.22	100	1.87	29	
	STDEV	0.49	0.04	0.20	0.10	0.03	0.06	0.17	0.17	0.10	0.03	0	0.83		Possible NDN 230 correlative
RS126															
	UA 2558_24	70.18	0.52	15.04	2.61	0.14	0.54	1.77	5.87	3.14	0.20	100	4.50		
	UA 2558_3	70.41	0.56	15.35	2.43	0.09	0.56	2.03	5.37	3.01	0.18	100	0.94		
	UA 2558_15	70.64	0.54	15.01	2.52	0.13	0.50	1.81	5.44	3.18	0.23	100	2.77		
	UA 2558_27	70.74	0.47	15.52	2.43	0.15	0.48	1.86	5.16	3.00	0.20	100	3.33		
	UA 2558_11	70.77	0.49	15.13	2.48	0.18	0.53	1.85	5.29	3.07	0.21	100	2.30		
	UA 2558_34	70.79	0.46	15.44	2.41	0.15	0.47	1.84	5.34	2.94	0.17	100	2.34		
	UA 2558_21	70.98	0.45	15.28	2.53	0.12	0.49	1.83	5.14	2.98	0.21	100	2.28		
	UA 2558_7	70.98	0.53	15.12	2.54	0.14	0.54	1.84	5.13	3.01	0.17	100	0.75		
	UA 2558_22	70.99	0.38	15.22	2.45	0.16	0.47	1.81	5.30	3.00	0.22	100	1.81		
	UA 2558_35	71.00	0.43	15.36	2.47	0.15	0.50	1.84	5.00	3.09	0.17	100	1.46		
	UA 2558_19	71.00	0.56	15.01	2.37	0.16	0.50	1.81	5.46	2.91	0.20	100	1.44		
	UA 2558_25	71.01	0.46	15.04	2.46	0.12	0.51	1.85	5.30	3.06	0.19	100	1.96		
	UA 2558_8	71.02	0.45	15.33	2.44	0.09	0.48	1.91	5.02	3.10	0.18	100	1.31		
	UA 2558_33	71.03	0.51	15.27	2.49	0.11	0.48	1.72	5.30	2.89	0.19	100	2.33		
	UA 2558_1	71.07	0.43	15.37	2.36	0.13	0.48	1.85	5.10	3.02	0.18	100	1.16		
	UA 2558_32	71.07	0.48	15.20	2.42	0.16	0.47	1.77	5.19	3.06	0.19	100	2.23		
	UA 2558_28	71.07	0.43	15.21	2.42	0.11	0.51	1.86	5.14	3.04	0.22	100	1.36		
	UA 2558_20	71.07	0.48	15.28	2.47	0.10	0.46	1.84	5.18	2.90	0.20	100	1.47		
	UA 2558_17	71.09	0.49	15.17	2.49	0.14	0.48	1.81	5.23	2.91	0.18	100	0.48		
	UA 2558_12	71.09	0.52	15.27	2.48	0.09	0.47	1.76	5.17	2.97	0.18	100	1.85		
	UA 2558_18	71.12	0.43	15.34	2.36	0.12	0.49	1.84	5.01	3.11	0.18	100	1.25		
	UA 2558_29	71.17	0.45	15.09	2.38	0.10	0.49	1.92	5.21	2.96	0.21	100	2.53		
	UA 2558_13	71.21	0.43	15.08	2.37	0.16	0.48	1.72	5.49	2.86	0.19	100	1.64		

	UA 2558_6	71.22	0.44	15.05	2.41	0.10	0.49	1.90	5.18	3.03	0.18	100	1.19	
	UA 2558_14	71.27	0.43	14.97	2.37	0.09	0.47	1.88	5.31	2.99	0.21	100	1.68	
	UA 2558_23	71.35	0.55	15.21	2.35	0.12	0.48	1.79	4.99	2.96	0.20	100	1.57	
	UA 2558_10	71.49	0.46	15.17	2.43	0.08	0.50	1.94	4.86	2.89	0.19	100	2.46	
	Mean	70.99	0.48	15.21	2.44	0.12	0.49	1.84	5.23	3.00	0.19	100	1.87	27
	STDEV	0.27	0.05	0.14	0.06	0.03	0.02	0.07	0.20	0.08	0.02	0	0.84	Aniakchak CFE II correlative
RS151														
	UA 2559_1	70.75	0.52	15.27	2.47	0.12	0.47	1.93	5.14	3.12	0.20	100	0.88	
	UA 2559_33	70.78	0.47	15.16	2.42	0.18	0.50	1.91	5.25	3.15	0.19	100	2.24	
	UA 2559_32	70.82	0.49	15.24	2.46	0.12	0.53	1.74	5.20	3.18	0.22	100	1.57	
	UA 2559_27	70.83	0.50	15.32	2.49	0.16	0.53	1.87	5.20	2.95	0.16	100	2.10	
	UA 2559_5	70.87	0.44	15.28	2.46	0.21	0.47	1.96	4.98	3.19	0.15	100	1.36	
	UA 2559_21	70.87	0.50	15.10	2.46	0.16	0.49	1.93	5.16	3.16	0.17	100	0.64	
	UA 2559_28	70.92	0.51	15.14	2.45	0.14	0.53	1.87	5.26	2.96	0.22	100	2.45	
	UA 2559_30	70.93	0.48	15.16	2.42	0.17	0.52	1.83	5.10	3.15	0.23	100	3.84	
	UA 2559_7	70.94	0.43	15.23	2.47	0.16	0.53	1.93	5.25	2.87	0.19	100	1.13	
	UA 2559_12	70.98	0.52	15.24	2.47	0.10	0.48	1.86	5.25	2.92	0.18	100	0.90	
	UA 2559_17	71.02	0.48	15.13	2.50	0.12	0.47	1.98	5.15	2.94	0.21	100	4.97	
	UA 2559_11	71.03	0.54	14.99	2.51	0.17	0.50	1.95	5.06	3.01	0.24	100	1.79	
	UA 2559_9	71.04	0.45	15.38	2.51	0.12	0.46	1.80	5.13	2.93	0.17	100	1.24	
	UA 2559_22	71.05	0.50	15.13	2.52	0.17	0.47	1.83	5.09	3.05	0.19	100	2.25	
	UA 2559_8	71.10	0.40	15.11	2.40	0.17	0.50	1.87	5.08	3.16	0.22	100	1.80	
	UA 2559_20	71.11	0.47	15.21	2.41	0.13	0.49	1.79	5.31	2.90	0.17	100	2.41	
	UA 2559_14	71.12	0.54	15.07	2.51	0.19	0.46	1.91	4.94	3.04	0.23	100	2.15	
	UA 2559_34	71.15	0.52	15.02	2.46	0.18	0.51	1.86	5.06	3.06	0.17	100	2.09	
	UA 2559_18	71.16	0.47	15.14	2.42	0.09	0.56	1.81	5.21	2.94	0.19	100	2.03	
	UA 2559_16	71.19	0.49	14.89	2.50	0.13	0.50	1.84	5.20	3.11	0.17	100	3.22	
	UA 2559_26	71.19	0.49	14.99	2.45	0.16	0.51	1.78	5.23	2.99	0.21	100	1.51	
	UA 2559_31	71.21	0.49	14.97	2.50	0.11	0.51	1.84	5.11	3.07	0.20	100	1.86	

	UA 2559_29	71.24	0.52	15.09	2.39	0.13	0.45	1.78	5.28	2.91	0.21	100	2.72		
	UA 2559_13	71.26	0.44	15.00	2.43	0.15	0.48	1.90	5.18	2.98	0.19	100	1.20		
	UA 2559_25	71.32	0.56	14.99	2.45	0.13	0.47	1.80	5.02	3.05	0.21	100	4.26		
	UA 2559_24	71.53	0.49	14.72	2.49	0.18	0.45	1.60	4.98	3.38	0.17	100	1.92		
	UA 2559_23	71.64	0.57	15.07	2.40	0.15	0.47	1.63	4.85	3.00	0.22	100	2.76		
	Mean	71.08	0.49	15.11	2.46	0.15	0.49	1.84	5.14	3.04	0.20	100	2.12	27	
	STDEV	0.21	0.04	0.14	0.04	0.03	0.03	0.09	0.11	0.12	0.02	0	1.02		Older Aniakchak correlative
WBP65															
	UA 2560_20	70.69	0.51	15.36	2.41	0.23	0.49	1.96	5.06	3.11	0.20	100	1.27		
	UA 2560_30	70.72	0.55	15.28	2.54	0.21	0.53	1.83	5.07	3.08	0.20	100	1.36		
	UA 2560_8	70.74	0.46	15.71	2.37	0.12	0.53	1.76	4.93	3.18	0.20	100	1.53		
	UA 2560_24	70.86	0.48	15.17	2.51	0.12	0.51	1.93	5.27	2.97	0.18	100	2.76		
	UA 2560_21	70.86	0.53	15.28	2.41	0.13	0.53	1.90	5.21	2.97	0.18	100	3.04		
	UA 2560_33	70.88	0.45	15.19	2.42	0.17	0.45	1.86	5.21	3.14	0.22	100	2.30		
	UA 2560_11	70.88	0.54	15.25	2.39	0.12	0.52	1.79	5.18	3.17	0.17	100	0.61		
	UA 2560_18	70.90	0.48	15.19	2.39	0.19	0.48	1.75	5.43	2.99	0.19	100	0.94		
	UA 2560_28	70.92	0.61	15.20	2.34	0.09	0.49	1.82	5.15	3.16	0.22	100	0.73		
	UA 2560_2	70.95	0.46	15.29	2.48	0.14	0.48	1.70	5.35	2.95	0.22	100	0.15		
	UA 2560_34	70.98	0.52	15.22	2.52	0.12	0.51	1.80	5.02	3.09	0.23	100	4.50		
	UA 2560_27	71.00	0.55	15.21	2.40	0.14	0.52	1.82	4.98	3.18	0.20	100	0.99		
	UA 2560_15	71.01	0.48	15.30	2.36	0.10	0.41	1.79	5.31	3.05	0.20	100	1.78		
	UA 2560_26	71.01	0.39	15.17	2.53	0.14	0.54	1.91	5.13	2.98	0.19	100	4.90		
	UA 2560_14	71.07	0.48	15.49	2.34	0.15	0.48	1.83	5.04	2.94	0.18	100	0.89		
	UA 2560_16	71.11	0.55	15.33	2.41	0.07	0.48	1.77	5.18	2.92	0.17	100	2.14		
	UA 2560_7	71.13	0.45	15.35	2.32	0.10	0.52	1.84	5.08	3.01	0.20	100	2.96		
	UA 2560_23	71.14	0.46	15.03	2.44	0.19	0.51	1.79	5.39	2.90	0.14	100	3.80		
	UA 2560_25	71.15	0.39	15.24	2.27	0.13	0.47	1.84	5.27	3.05	0.21	100	1.13		
	UA 2560_4	71.15	0.44	15.15	2.43	0.16	0.53	1.85	5.14	2.99	0.18	100	2.08		
	UA 2560_22	71.19	0.46	15.22	2.40	0.13	0.50	1.80	5.07	3.05	0.17	100	2.89		

	UA 2560_17	71.19	0.50	15.04	2.40	0.11	0.49	1.82	5.04	3.21	0.20	100	1.11		
	UA 2560_32	71.19	0.53	15.16	2.50	0.09	0.45	1.77	5.20	2.91	0.19	100	1.20		
	UA 2560_19	71.20	0.50	15.06	2.41	0.14	0.52	1.74	5.24	2.99	0.21	100	2.09		
	UA 2560_6	71.20	0.41	15.20	2.47	0.15	0.50	1.81	5.04	3.01	0.20	100	1.37		
	UA 2560_9	71.23	0.50	15.25	2.34	0.10	0.50	1.76	5.16	2.97	0.20	100	0.02		
	UA 2560_10	71.25	0.51	14.97	2.38	0.18	0.50	1.73	5.09	3.14	0.23	100	4.68		
	UA 2560_1	71.31	0.49	15.11	2.51	0.16	0.48	1.75	5.21	2.78	0.20	100	2.41		
	UA 2560_35	71.32	0.54	15.12	2.35	0.15	0.53	1.74	5.03	3.05	0.18	100	0.67		
	UA 2560_12	71.33	0.47	15.12	2.44	0.13	0.53	1.76	5.04	3.00	0.19	100	4.68		
	UA 2560_29	71.35	0.52	15.24	2.38	0.14	0.55	1.77	4.99	2.90	0.17	100	2.24		
	UA 2560_13	71.40	0.42	15.28	2.31	0.16	0.52	1.77	4.80	3.16	0.18	100	1.10		
	UA 2560_3	71.42	0.41	15.04	2.50	0.13	0.51	1.71	5.15	2.95	0.18	100	1.36		
	UA 2560_31	71.50	0.49	15.14	2.27	0.16	0.53	1.76	5.10	2.88	0.17	100	1.65		
	Mean	71.09	0.49	15.22	2.41	0.14	0.50	1.80	5.13	3.02	0.19	100	1.98	34	
	STDEV	0.21	0.05	0.14	0.07	0.03	0.03	0.06	0.13	0.10	0.02	0	1.32		Aniakchak CFE II correlative
RC127															
	UA 2561_12	70.49	0.46	15.24	2.46	0.17	0.54	2.16	5.28	3.03	0.18	100	0.79		
	UA 2561_17	70.69	0.50	15.20	2.38	0.14	0.46	2.23	5.22	3.00	0.18	100	1.31		
	UA 2561_6	70.81	0.43	15.22	2.42	0.17	0.49	2.00	5.28	2.99	0.21	100	0.66		
	UA 2561_11	70.91	0.51	15.15	2.50	0.13	0.52	2.12	4.93	3.02	0.20	100	1.65		
	UA 2561_35	70.92	0.50	15.16	2.34	0.14	0.46	2.08	5.17	3.04	0.18	100	1.55		
	UA 2561_8	70.92	0.48	15.22	2.46	0.14	0.47	2.18	4.85	3.09	0.20	100	0.73		
	UA 2561_15	70.94	0.45	15.21	2.47	0.10	0.49	2.16	5.05	2.94	0.19	100	1.79		
	UA 2561_7	70.97	0.53	15.06	2.40	0.16	0.53	2.08	5.13	2.96	0.20	100	1.49		
	UA 2561_16	70.97	0.47	15.03	2.38	0.06	0.50	2.11	5.29	3.01	0.18	100	1.53		
	UA 2561_4	70.98	0.51	15.36	2.38	0.12	0.46	2.00	5.04	2.94	0.21	100	1.85		
	UA 2561_5	70.98	0.44	14.88	2.48	0.12	0.49	2.02	5.35	3.02	0.21	100	2.00		
	UA 2561_31	71.01	0.43	15.29	2.28	0.13	0.53	2.05	5.00	3.10	0.18	100	0.98		
	UA 2561_1	71.04	0.50	15.13	2.39	0.15	0.49	2.07	4.98	3.04	0.22	100	1.11		

	UA 2561_29	71.09	0.45	15.19	2.32	0.13	0.44	2.07	5.25	2.92	0.17	100	2.83		
	UA 2561_19	71.10	0.45	15.07	2.35	0.12	0.46	2.07	5.23	2.94	0.21	100	1.96		
	UA 2561_27	71.12	0.46	15.15	2.43	0.14	0.46	2.02	5.09	2.91	0.20	100	2.94		
	UA 2561_2	71.13	0.45	15.19	2.44	0.14	0.48	2.00	4.98	2.95	0.23	100	3.60		
	UA 2561_14	71.14	0.46	15.01	2.41	0.15	0.49	2.06	5.09	3.03	0.17	100	2.87		
	UA 2561_13	71.15	0.45	14.96	2.30	0.15	0.48	2.09	5.15	3.08	0.21	100	1.67		
	UA 2561_32	71.16	0.52	15.22	2.35	0.12	0.47	2.01	5.01	2.92	0.22	100	0.56		
	UA 2561_33	71.17	0.44	15.25	2.36	0.15	0.49	2.11	4.83	3.04	0.16	100	1.27		
	UA 2561_34	71.17	0.55	15.09	2.33	0.15	0.46	2.01	5.01	3.04	0.20	100	2.12		
	UA 2561_22	71.24	0.46	15.11	2.36	0.15	0.48	2.04	5.01	2.98	0.19	100	1.28		
	UA 2561_10	71.26	0.46	15.18	2.43	0.12	0.49	2.09	4.96	2.81	0.21	100	2.52		
	UA 2561_28	71.31	0.48	15.00	2.32	0.12	0.43	2.14	5.16	2.86	0.17	100	1.70		
	UA 2561_20	71.32	0.50	15.00	2.45	0.18	0.48	2.00	4.92	2.96	0.20	100	0.77		
	UA 2561_18	71.38	0.46	15.02	2.29	0.13	0.48	1.87	5.16	3.06	0.15	100	2.03		
	UA 2561_26	71.41	0.48	14.94	2.43	0.11	0.48	1.94	5.13	2.93	0.17	100	1.73		
	Mean	71.06	0.47	15.13	2.39	0.13	0.48	2.06	5.09	2.99	0.19	100	1.69	28	
	STDEV	0.20	0.03	0.11	0.06	0.02	0.03	0.08	0.14	0.07	0.02	0	0.76		Aniakchak CFE II correlative
RC108															
	UA 2563_1	74.10	0.32	14.15	1.92	0.13	0.45	2.61	4.22	1.89	0.21	100	3.28		
	UA 2563_2	74.04	0.36	13.96	1.65	0.07	0.44	2.55	4.73	2.01	0.20	100	1.82		
	UA 2563_4	74.22	0.24	13.77	1.87	0.15	0.44	2.57	4.43	2.11	0.21	100	2.31		
	UA 2563_6	73.78	0.32	13.92	1.97	0.07	0.51	2.72	4.44	2.08	0.20	100	0.80		
	Mean	74.03	0.31	13.95	1.85	0.10	0.46	2.61	4.46	2.02	0.20	100	2.05	4	
	STDEV	0.19	0.05	0.16	0.14	0.04	0.03	0.07	0.21	0.10	0.01	0	1.03		Possible NDN 230 correlative
UA 1602															
	UA 1602_35	55.81	1.28	16.22	8.50	0.23	3.12	9.40	3.97	1.31	0.15	100	0.51		
	UA 1602_29	56.43	1.39	15.86	7.84	0.26	3.05	9.17	4.52	1.36	0.11	100	0.05		

	UA 1602_7	56.63	1.39	15.83	8.22	0.21	2.96	8.79	4.36	1.46	0.14	100	-1.40		
	UA 1602_33	57.03	1.28	15.86	7.93	0.26	2.82	8.86	4.35	1.49	0.11	100	-0.80		
	UA 1602_1	57.04	1.31	16.08	8.17	0.17	2.98	8.64	4.05	1.47	0.08	100	-0.19		
	UA 1602_2	57.30	1.29	16.48	7.50	0.15	2.93	8.34	4.32	1.57	0.13	100	0.09		
	UA 1602_3	58.29	1.37	16.39	7.32	0.17	2.89	7.72	4.09	1.65	0.11	100	-0.26		
	UA 1602_31	58.51	1.33	16.00	7.16	0.21	2.70	8.06	4.39	1.56	0.09	100	1.73		
	UA 1602_34	58.85	1.15	16.18	6.86	0.28	2.53	7.81	4.61	1.60	0.12	100	-0.61		
	UA 1602_27	58.92	1.30	16.07	6.92	0.19	2.62	7.66	4.49	1.71	0.13	100	0.92		
	UA 1602_32	59.90	1.09	16.18	6.56	0.15	2.50	7.26	4.38	1.87	0.12	100	0.75		
	UA 1602_40	64.00	1.12	15.25	5.78	0.16	1.58	5.14	4.36	2.49	0.13	100	0.43		
	Mean	58.23	1.27	16.03	7.40	0.20	2.72	8.07	4.32	1.63	0.12	100	0.10	12	
	STDEV	2.18	0.10	0.32	0.79	0.05	0.41	1.13	0.19	0.31	0.02	0	0.84		Aniakchak CFE II (pop 1)
UA 1602															
	UA 1602_30	70.53	0.49	15.30	2.53	0.12	0.46	2.09	5.26	3.00	0.21	100	0.13		
	UA 1602_24	70.69	0.55	15.11	2.56	0.13	0.54	2.21	5.00	3.03	0.18	100	1.59		
	UA 1602_4	70.72	0.41	15.12	2.57	0.12	0.55	2.17	5.12	3.00	0.21	100	1.54		
	UA 1602_18	70.76	0.46	15.14	2.54	0.12	0.49	2.06	5.14	3.09	0.20	100	1.70		
	UA 1602_28	70.83	0.49	15.23	2.46	0.21	0.47	2.08	5.03	2.96	0.23	100	2.73		
	UA 1602_14	70.86	0.44	15.25	2.37	0.09	0.47	2.12	5.09	3.08	0.22	100	0.46		
	UA 1602_8	70.88	0.54	15.17	2.56	0.12	0.50	2.13	5.01	2.87	0.21	100	5.09		
	UA 1602_5	70.91	0.45	15.26	2.46	0.17	0.48	2.03	4.98	3.07	0.18	100	-0.20		
	UA 1602_26	70.92	0.49	15.03	2.44	0.13	0.49	2.04	5.09	3.16	0.20	100	0.95		
	UA 1602_13	70.94	0.47	15.19	2.38	0.13	0.52	2.04	5.14	3.00	0.18	100	0.21		
	UA 1602_21	70.98	0.43	15.04	2.41	0.19	0.48	2.21	5.12	2.98	0.15	100	1.42		
	UA 1602_19	71.02	0.47	14.89	2.41	0.17	0.50	2.08	5.21	3.04	0.20	100	1.97		
	UA 1602_16	71.03	0.42	15.15	2.48	0.11	0.48	2.10	5.03	3.00	0.19	100	0.06		
	UA 1602_38	71.10	0.44	15.20	2.48	0.10	0.45	2.06	5.00	2.97	0.20	100	3.32		
	UA 1602_39	71.11	0.48	15.23	2.48	0.11	0.56	1.89	4.88	3.08	0.18	100	2.14		
	UA 1602_11	71.17	0.48	15.12	2.51	0.13	0.50	1.96	4.99	2.97	0.17	100	2.96		

	UA 1602_25	71.18	0.43	15.00	2.42	0.14	0.49	1.92	5.30	2.95	0.17	100	1.79		
	UA 1602_23	71.19	0.47	14.94	2.52	0.16	0.50	2.06	5.06	2.93	0.18	100	2.28		
	UA 1602_12	71.23	0.53	15.08	2.48	0.12	0.51	2.05	4.89	2.93	0.18	100	2.58		
	UA 1602_22	71.23	0.51	15.05	2.36	0.06	0.48	2.12	5.11	2.89	0.21	100	1.38		
	UA 1602_15	71.68	0.39	15.01	2.35	0.12	0.52	1.96	4.70	3.09	0.19	100	1.23		
	Mean	71.00	0.47	15.12	2.47	0.13	0.50	2.07	5.06	3.00	0.19	100	1.68	21	
	STDEV	0.25	0.04	0.11	0.07	0.03	0.03	0.08	0.13	0.07	0.02	0	1.26		Aniakchak CFE II (pop 2)
NDN 230															
	NDN-230	73.78	0.32	13.93	2.12	0.11	0.53	2.55	4.58	2.03	0.05	100.00	1.71		
	NDN-230	73.84	0.29	13.68	2.13	0.09	0.56	2.36	4.89	2.08	0.08	100.00	1.47		
	NDN-230	73.97	0.30	13.89	1.97	0.10	0.51	2.43	4.60	2.14	0.06	100.00	0.68		
	NDN-230	74.03	0.30	13.79	2.06	0.09	0.49	2.51	4.62	2.03	0.07	100.00	0.94		
	NDN-230	74.13	0.30	13.71	2.19	0.11	0.48	2.30	4.74	1.98	0.06	100.00	-0.32		
	NDN-230	74.15	0.32	13.79	2.03	0.10	0.48	2.31	4.71	2.04	0.07	100.00	1.90		
	NDN-230	74.33	0.31	13.88	1.90	0.11	0.54	2.17	4.81	1.89	0.06	100.00	1.07		
	NDN-230	74.36	0.31	13.54	1.92	0.10	0.55	2.32	4.67	2.17	0.06	100.00	0.99		
	NDN-230	74.39	0.31	13.69	2.02	0.11	0.49	2.28	4.65	2.00	0.06	100.00	1.19		
	NDN-230	74.39	0.31	13.74	1.97	0.11	0.50	2.42	4.60	1.90	0.06	100.00	1.08		
	NDN-230	74.50	0.31	13.93	1.86	0.10	0.49	2.21	4.53	2.02	0.06	100.00	0.71		
	NDN-230	74.56	0.28	13.79	2.01	0.10	0.45	2.13	4.57	2.03	0.06	100.00	0.66		
	NDN-230	74.56	0.30	13.75	1.80	0.10	0.45	2.29	4.44	2.26	0.05	100.00	-0.25		
	NDN-230	74.69	0.31	13.66	1.97	0.09	0.46	2.21	4.40	2.14	0.06	100.00	0.84		
	NDN-230	74.86	0.29	13.55	1.95	0.09	0.48	2.28	4.57	1.89	0.06	100.00	1.29		
	NDN-230	74.96	0.27	13.33	1.87	0.10	0.44	2.12	4.63	2.23	0.05	100.00	1.45		
	NDN-230	74.98	0.30	13.63	1.78	0.10	0.45	2.31	4.48	1.92	0.04	100.00	0.84		
	NDN-230	74.98	0.31	13.34	2.06	0.10	0.44	2.30	4.57	1.83	0.07	100.00	1.94		
	NDN-230	75.10	0.29	13.51	1.95	0.10	0.42	2.16	4.43	2.02	0.04	100.00	0.35		Data produced at the University
	NDN-230	75.24	0.31	13.74	1.78	0.11	0.50	2.28	4.07	1.91	0.05	100.00	1.78		of Edinburgh
	Mean	74.49	0.30	13.69	1.97	0.10	0.48	2.30	4.58	2.03	0.06	100.00	1.02	20	Pyne O'Donnell *et al.*, (2012)

	STDEV	0.43	0.01	0.17	0.12	0.01	0.04	0.12	0.17	0.12	0.01	0.00	0.63	
Hayes F2														
	UA 2614-4	71.64	0.20	15.94	1.68	0.09	0.44	3.28	4.17	2.27	0.39	100	4.41	
	UA 2614-9	71.96	0.40	14.37	2.48	0.10	1.26	2.77	3.88	2.44	0.43	100	3.07	
	UA 2614-44	72.16	0.29	15.20	2.03	0.15	0.45	2.51	4.25	2.62	0.43	100	4.00	
	UA 2614-30	73.17	0.27	14.76	1.74	0.10	0.53	2.31	4.18	2.64	0.38	100	4.31	
	UA 2614-3	73.34	0.27	14.71	1.87	0.06	0.50	2.32	4.05	2.57	0.41	100	4.65	
	UA 2614-43	73.39	0.27	14.55	1.99	0.03	0.49	2.19	3.99	2.75	0.45	100	3.15	
	UA 2614-5	73.39	0.19	14.86	1.77	0.07	0.44	2.24	4.15	2.61	0.37	100	4.80	
	UA 2614-25	73.42	0.27	14.86	1.71	0.10	0.46	2.21	3.91	2.75	0.40	100	1.73	
	UA 2614-15	73.66	0.21	14.60	1.73	0.09	0.45	2.10	4.23	2.64	0.38	100	3.37	
	UA 2614-36	73.67	0.25	14.49	1.79	0.07	0.48	2.21	3.99	2.76	0.35	100	3.35	
	UA 2614-19	73.81	0.27	14.78	1.62	0.08	0.42	2.10	3.92	2.73	0.33	100	5.44	
	UA 2614-6	73.91	0.18	14.76	1.74	0.10	0.47	2.16	3.90	2.58	0.28	100	1.68	
	UA 2614-7	73.92	0.17	14.47	1.80	0.12	0.48	2.25	3.99	2.53	0.34	100	2.92	
	UA 2614-23	74.01	0.22	14.51	1.60	0.06	0.48	2.13	4.05	2.63	0.40	100	2.74	
	UA 2614-39	74.06	0.18	14.54	1.85	0.03	0.44	2.22	3.87	2.52	0.38	100	3.81	
	UA 2614-24	74.17	0.20	14.49	1.65	0.11	0.45	2.10	3.92	2.61	0.41	100	2.78	
	UA 2614-35	74.25	0.19	14.37	1.78	0.12	0.42	2.25	4.15	2.26	0.28	100	2.47	
	UA 2614-8	74.25	0.18	14.28	1.64	0.12	0.43	2.11	4.07	2.63	0.39	100	3.27	
	UA 2614-20	74.35	0.22	14.37	1.69	0.09	0.43	2.20	3.78	2.61	0.33	100	3.64	
	UA 2614-26	74.58	0.20	14.27	1.57	0.06	0.42	2.16	3.97	2.50	0.35	100	5.64	
	UA 2614-14	74.75	0.22	14.33	1.52	0.08	0.41	1.96	3.81	2.66	0.33	100	4.36	
	UA 2614-3	74.77	0.23	14.16	1.51	0.03	0.36	1.95	3.90	2.84	0.32	100	5.74	
	UA 2614-31	74.77	0.18	14.72	1.06	0.07	0.25	1.79	4.13	2.82	0.27	100	3.60	
	UA 2614-11	74.85	0.25	14.19	1.49	0.02	0.42	1.92	3.96	2.69	0.27	100	4.15	
	Mean	73.76	0.23	14.61	1.72	0.08	0.47	2.23	4.01	2.61	0.36	100	3.71	24 Davies *et al.,* (2016)
	STDEV	0.87	0.05	0.38	0.25	0.03	0.18	0.30	0.13	0.15	0.05	0	1.10	

White River Ash east

UA 1119	71.28	0.24	15.40	1.85	0.10	0.31	2.26	4.56	3.66	0.35	100	1.05
UA 1119	71.46	0.00	15.14	2.25	0.02	0.55	2.10	4.78	3.16	0.54	100	0.88
UA 1119	71.56	0.23	15.68	1.71	0.03	0.28	2.35	4.31	3.48	0.38	100	2.08
UA 1119	71.57	0.14	16.09	1.55	0.03	0.29	2.51	5.16	2.47	0.19	100	1.52
UA 1119	71.87	0.29	15.88	1.94	-0.05	0.48	1.72	4.61	2.87	0.41	100	4.44
UA 1119	72.27	0.39	15.09	1.82	0.20	0.62	2.10	4.59	2.66	0.24	100	0.61
UA 1119	72.43	0.24	14.60	2.25	0.14	0.23	2.14	4.15	3.36	0.47	100	4.63
UA 1119	72.49	0.38	15.13	1.53	0.20	0.41	1.61	4.42	3.36	0.47	100	3.97
UA 1119	72.57	0.13	14.01	2.48	0.03	0.79	2.34	4.42	2.85	0.37	100	1.39
UA 1119	72.61	0.17	13.51	1.96	-0.15	0.75	2.37	4.58	3.93	0.27	100	0.89
UA 1119	72.63	0.28	14.39	2.22	-0.11	0.37	1.92	4.34	3.62	0.34	100	1.72
UA 1119	72.65	0.18	15.28	1.20	0.26	0.67	1.90	4.49	3.10	0.27	100	0.82
UA 1119	72.66	0.11	14.88	1.55	0.85	0.73	1.62	4.37	2.80	0.42	100	1.34
UA 1119	72.67	0.07	14.92	1.96	0.03	0.39	1.81	4.80	3.01	0.34	100	-0.14
UA 1119	72.74	0.20	14.46	2.04	0.20	0.19	1.99	4.85	2.93	0.41	100	1.95
UA 1119	72.80	0.12	14.84	1.32	0.10	0.21	2.05	4.05	4.02	0.50	100	-0.15
UA 1119	72.84	-0.03	15.59	2.06	-0.18	0.34	2.29	3.97	2.92	0.20	100	0.29
UA 1119	72.96	0.27	15.11	1.60	0.01	0.38	2.22	4.29	2.90	0.25	100	3.12
UA 1119	73.04	0.12	14.58	1.32	-0.03	0.86	2.27	4.47	3.06	0.31	100	4.78
UA 1119	73.05	0.29	15.12	1.40	0.03	0.32	1.78	4.79	2.96	0.25	100	1.93
UA 1119	73.12	0.02	15.37	1.40	0.04	0.25	2.10	4.18	3.18	0.33	100	-0.59
UA 1119	73.19	0.23	14.12	1.27	0.16	0.41	2.55	4.60	3.08	0.39	100	3.48
UA 1119	73.23	0.27	14.50	1.75	-0.03	0.70	1.68	4.29	3.30	0.31	100	4.92
UA 1119	73.27	0.06	14.03	2.03	-0.11	0.47	1.93	4.37	3.64	0.32	100	3.02
UA 1119	73.32	0.18	14.66	1.66	0.25	0.25	1.67	4.10	3.45	0.46	100	2.62
UA 1119	73.38	0.21	14.41	1.76	0.07	0.37	2.03	4.29	3.12	0.36	100	1.24
UA 1119	73.39	0.26	14.62	1.91	0.10	0.37	2.05	3.94	2.96	0.39	100	1.87
UA 1119	73.49	0.26	13.66	1.58	0.03	0.14	2.57	4.96	3.09	0.23	100	1.18

UA 1119	73.52	0.20	14.41	1.66	0.07	0.39	2.03	4.30	3.03	0.40	100	2.47
UA 1119	73.53	0.42	13.65	1.73	0.10	0.23	1.91	4.59	3.58	0.27	100	3.06
UA 1119	73.54	0.35	13.33	1.68	0.08	1.38	2.35	4.08	2.88	0.34	100	4.19
UA 1119	73.55	0.24	14.55	1.62	0.01	0.42	1.95	4.07	3.26	0.33	100	3.50
UA 1119	73.56	0.28	14.26	1.59	0.03	0.38	2.06	4.49	2.99	0.36	100	2.69
UA 1119	73.57	0.00	14.77	1.23	-0.05	0.52	2.08	4.25	3.35	0.29	100	1.38
UA 1119	73.58	0.28	14.60	1.52	0.08	0.39	1.86	4.22	3.13	0.33	100	3.00
UA 1119	73.67	0.17	14.42	1.53	0.06	0.38	1.95	4.17	3.27	0.36	100	1.70
UA 1119	73.67	0.07	14.46	1.64	-0.14	0.47	2.08	4.37	2.95	0.43	100	2.56
UA 1119	73.69	0.17	14.54	1.57	0.03	0.41	1.99	4.17	3.11	0.33	100	3.14
UA 1119	73.74	0.20	14.65	1.39	0.06	0.24	1.87	4.37	3.17	0.30	100	2.35
UA 1119	73.76	0.08	14.54	1.26	0.26	0.11	1.88	3.95	3.80	0.36	100	3.79
UA 1119	73.78	0.35	13.96	1.36	0.04	0.84	1.70	4.34	3.24	0.39	100	2.31
UA 1119	73.93	0.29	14.10	1.43	0.07	0.13	1.53	4.30	4.00	0.24	100	3.77
UA 1119	73.94	0.21	14.32	1.53	0.03	0.46	1.81	4.21	3.16	0.33	100	2.30
UA 1119	73.94	0.30	13.71	1.90	0.14	0.26	1.79	4.95	2.69	0.32	100	2.93
UA 1119	73.98	0.50	14.10	1.44	0.05	0.33	1.75	4.24	3.25	0.37	100	2.40
UA 1119	73.99	0.25	14.20	1.63	-0.05	0.43	1.64	4.27	3.38	0.26	100	1.27
UA 1119	74.04	0.08	14.14	1.49	0.12	0.37	1.74	4.55	2.99	0.48	100	2.24
UA 1119	74.07	0.15	13.65	1.64	0.34	0.21	1.63	4.17	3.74	0.38	100	3.12
UA 1119	74.14	0.12	13.46	2.08	0.09	0.25	1.60	4.54	3.48	0.24	100	2.50
UA 1119	74.23	0.32	14.35	1.50	0.05	0.31	1.85	3.66	3.39	0.34	100	2.77
UA 1119	74.32	0.15	13.41	1.87	-0.05	0.27	1.87	4.19	3.64	0.32	100	2.25
UA 1119	74.35	0.16	14.21	1.47	0.04	0.24	1.66	4.21	3.33	0.32	100	3.57
UA 1119	74.39	0.14	14.05	1.41	-0.23	0.42	1.88	4.43	3.11	0.41	100	2.68
UA 1119	74.41	0.20	14.11	1.41	0.07	0.31	1.67	4.20	3.31	0.31	100	3.79
UA 1119	74.43	0.02	13.83	1.30	0.55	0.00	1.59	4.22	3.78	0.30	100	2.03
UA 1119	74.49	0.22	14.24	1.27	0.01	0.32	1.59	4.19	3.36	0.31	100	1.95
UA 1119	74.49	0.40	14.19	1.01	0.24	0.27	1.44	4.23	3.09	0.63	100	2.53
UA 1119	74.49	0.14	13.52	1.64	-0.07	0.33	1.93	4.70	3.02	0.30	100	2.91

	UA 1119	74.56	-0.03	14.54	1.30	-0.04	0.07	1.66	4.27	3.41	0.26	100	1.78		
	UA 1119	74.66	0.15	14.65	1.93	-0.25	0.34	1.84	3.43	2.85	0.40	100	2.57		
	UA 1119	74.77	0.15	13.39	1.44	0.08	0.14	1.85	4.06	3.78	0.33	100	3.34		
	UA 1119	74.88	0.18	13.57	1.42	0.36	0.45	1.83	4.33	2.70	0.28	100	3.16		
	UA 1119	74.90	0.00	13.89	1.50	0.17	0.11	1.60	3.45	4.05	0.32	100	2.68		
	UA 1119	74.91	0.00	14.62	1.47	-0.15	0.14	1.62	4.06	2.97	0.35	100	3.89		
	UA 1119	74.98	0.23	13.81	1.12	-0.14	0.72	1.11	4.33	3.56	0.28	100	1.44		
	UA 1119	75.06	0.24	13.70	0.74	-0.07	0.22	1.59	4.67	3.44	0.42	100	3.96		
	UA 1119	75.12	0.18	14.37	1.49	-0.07	0.21	1.52	3.99	2.95	0.24	100	1.81		
	UA 1119	75.12	0.07	13.09	2.06	-0.17	0.36	1.74	4.41	3.06	0.26	100	3.62		
	UA 1119	75.31	0.16	13.79	1.20	0.04	0.23	1.54	4.00	3.43	0.31	100	3.33		
	Mean:	73.65	0.19	14.34	1.60	0.07	0.38	1.91	4.31	3.21	0.34	100	2.91	69	
	SD:	0.97	0.12	0.63	0.33	0.20	0.22	0.30	0.31	0.36	0.08	0	1.73		Jensen *et al.,* (2014)
White River Ash north															
	UA 1046	72.38	0.21	14.85	1.96	0.11	0.44	2.43	4.06	3.17	0.39	100	1.16		
	UA 1046	72.38	0.24	15.03	1.86	0.07	0.38	2.30	4.32	3.05	0.37	100	1.72		
	UA 1046	72.10	0.24	14.86	1.94	0.10	0.48	2.32	4.52	3.07	0.36	100	4.10		
	UA 1046	72.37	0.20	15.10	1.88	0.05	0.40	2.30	4.30	3.08	0.32	100	2.28		
	UA 1046	72.18	0.27	14.85	1.99	0.08	0.47	2.35	4.20	3.22	0.38	100	3.48		
	UA 1046	73.05	0.19	15.23	1.96	0.07	0.44	2.40	3.17	3.06	0.42	100	3.30		
	UA 1046	73.94	0.22	14.98	1.69	0.04	0.45	2.23	3.03	3.03	0.39	100	3.23		
	UA 1046	73.76	0.24	14.09	1.66	0.07	0.41	1.87	4.02	3.49	0.38	100	2.64		
	UA 1046	72.46	0.27	15.44	1.87	0.06	0.48	2.61	3.56	2.90	0.36	100	2.11		
	UA 1046	72.19	0.21	15.24	1.86	0.05	0.41	2.26	4.33	3.08	0.36	100	2.28		
	UA 1046	71.88	0.33	15.58	1.90	0.04	0.35	2.41	4.21	2.96	0.33	100	2.48		
	UA 1046	72.27	0.26	14.85	1.77	0.09	0.45	2.39	4.31	3.17	0.44	100	4.23		
	UA 1046	72.30	0.25	15.10	1.93	0.09	0.50	2.27	4.09	3.19	0.28	100	1.35		

UA 1046	70.74	0.30	15.96	1.80	0.07	0.37	2.84	4.79	2.82	0.31	100	1.58	
UA 1046	75.47	0.14	13.57	1.47	0.02	0.27	1.40	4.01	3.34	0.31	100	1.71	
UA 1046	72.44	0.24	15.03	1.88	0.02	0.44	2.30	4.33	2.98	0.33	100	1.84	
UA 1046	75.10	0.13	13.33	1.11	0.04	0.27	1.92	4.55	3.26	0.28	100	1.92	
UA 1046	75.63	0.18	13.64	1.24	0.06	0.24	1.46	4.17	3.14	0.26	100	2.38	
UA 1046	72.48	0.21	15.15	1.78	0.06	0.37	2.21	4.43	2.96	0.36	100	1.94	
UA 1046	72.64	0.29	15.12	1.88	0.03	0.43	2.14	4.21	2.91	0.35	100	1.47	
UA 1046	75.28	0.10	14.22	0.93	0.05	0.08	1.73	4.38	3.01	0.22	100	2.07	
UA 1046	72.30	0.23	15.15	1.80	0.02	0.39	2.26	4.38	3.14	0.32	100	1.98	
UA 1046	72.52	0.34	15.27	1.82	0.06	0.35	2.21	4.03	3.06	0.32	100	2.13	
UA 1046	75.35	0.20	14.01	1.32	0.05	0.22	1.39	3.99	3.24	0.23	100	1.57	
UA 1046	75.83	0.08	13.74	1.24	0.04	0.21	1.40	3.93	3.27	0.27	100	0.75	
UA 1046	72.09	0.30	14.72	2.15	0.03	0.43	2.25	4.30	3.32	0.40	100	4.48	
UA 1046	72.15	0.26	15.15	1.88	0.08	0.45	2.39	4.34	2.95	0.34	100	1.87	
UA 1046	72.45	0.28	15.21	1.85	0.05	0.38	2.19	4.30	2.93	0.35	100	1.54	
UA 1046	72.10	0.17	15.26	1.87	0.06	0.41	2.37	4.33	3.09	0.34	100	1.88	
UA 1046	72.10	0.24	15.00	1.98	0.03	0.46	2.44	4.34	3.04	0.38	100	1.25	
UA 1046	72.18	0.20	15.29	1.84	0.06	0.39	2.38	4.31	3.04	0.31	100	1.57	
UA 1046	74.56	0.05	14.67	0.94	0.07	0.02	1.87	4.69	2.89	0.25	100	1.23	
Mean:	73.02	0.22	14.83	1.72	0.06	0.37	2.17	4.19	3.09	0.33	100	2.17	32
SD:	1.35	0.07	0.62	0.32	0.02	0.11	0.36	0.37	0.15	0.05	0	0.92	Davies et al. (2016)

Table S2: Operating conditions and glass chemistry produced at the University of Oxford
Data normalised to 100%. STDEV = standard deviation.

Operating conditions: Samples were run on a JEOL-8600 wavelength-dispersive electron microprobe at the Research Laboratory for Archaeology and the History of Art, University of Oxford. 11 elements were measured (Si, Ti, Al, Fe, Mn, Mg, Ca, Na, K, Cl, P) using a 10 micron beam and 6 nA beam current, with an accelerating voltage of 15 kV. Peak counting times were 30s for Si, Al, Fe, Ca, K and Ti; 40s for Cl and Mn; 60s for P; and 10s for Na. The MPI-DING reference glasses were run as secondary standards and results were within 1 standard deviation of the preferred values (Jochum *et al.,* 2006).

Tephra	Sample	SiO_2	TiO2	Al_2O_3	FeO_T	MnO	MgO	CaO	Na_2O	K_2O	Cl	P2O5	Total	H2O Diff	n	Comments/ Correlations
J127																
	J127_37	76.23	0.30	13.19	1.58	0.03	0.37	2.21	4.21	1.58	0.24	0.05	100	1.07		
	J127_32	76.39	0.26	12.98	1.41	0.05	0.39	2.40	4.15	1.65	0.28	0.05	100	3.13		
	J127_28	76.44	0.31	12.99	1.51	0.11	0.31	2.32	4.09	1.69	0.19	0.02	100	1.24		
	J127_29	76.47	0.28	12.83	1.59	0.10	0.35	2.16	4.23	1.70	0.28	0.01	100	3.03		
	J127_1	76.63	0.31	13.02	1.42	0.05	0.39	2.16	3.99	1.67	0.27	0.08	100	3.89		
	J127_8	76.84	0.22	12.78	1.48	0.08	0.41	2.13	4.05	1.62	0.38	0.01	100	4.63		
	J127_30	76.84	0.28	12.80	1.47	0.11	0.33	2.15	4.04	1.63	0.32	0.03	100	5.32		
	J127_40	76.95	0.29	13.35	1.53	0.05	0.42	2.33	3.09	1.70	0.23	0.05	100	3.69		
	J127_12	77.73	0.26	12.63	1.40	0.10	0.32	1.62	4.04	1.64	0.24	0.02	100	2.03		
	Mean	76.72	0.28	12.95	1.49	0.08	0.37	2.16	3.99	1.66	0.27	0.04	100	3.11	9	Possible Mt. Augustine/
	STDEV	0.45	0.03	0.22	0.07	0.03	0.04	0.23	0.34	0.04	0.05	0.02	0	1.46		Mt. Kuygak correlative
J184																
	JHT_33	63.94	1.27	15.05	5.70	0.18	2.32	4.56	4.13	2.37	0.14	0.35	100	2.98		
	JHT_9	66.89	1.45	13.57	5.52	0.08	1.19	2.99	3.70	4.13	0.06	0.43	100	4.41		
	JHT_13	67.65	1.23	14.47	4.41	0.11	1.41	3.67	3.90	2.76	0.08	0.30	100	2.39		
	JHT_25	68.06	1.21	14.77	4.52	0.06	1.40	3.96	2.87	2.76	0.11	0.31	100	0.51		
	JHT_3	68.18	0.90	15.50	2.95	0.02	0.73	2.97	4.77	3.70	0.11	0.18	100	3.48		
	JHT_34	68.47	1.06	14.17	4.31	0.06	0.90	2.47	4.27	3.99	0.07	0.23	100	3.88		

	JHT_30	69.47	0.60	16.94	1.40	0.00	0.48	3.07	4.98	2.84	0.07	0.16	100	2.17		
	JHT_39	69.81	1.65	12.78	4.40	0.13	0.40	1.61	3.77	4.92	0.04	0.50	100	2.93		
	JHT_38	70.22	0.52	15.12	2.62	0.04	0.15	1.33	5.20	4.52	0.15	0.12	100	1.66		
	JHT_15	70.55	0.66	15.37	2.22	0.02	0.37	3.24	4.15	3.18	0.11	0.15	100	2.29		
	JHT_26	70.97	1.42	13.77	3.15	0.02	0.22	1.36	4.55	4.09	0.16	0.30	100	4.59		
	JHT_22	71.98	0.92	13.30	3.19	0.06	0.53	1.78	3.99	3.97	0.12	0.15	100	1.35		
	JHT_20	72.05	0.62	14.60	1.87	0.07	0.30	2.72	4.40	3.14	0.05	0.18	100	4.54		
	JHT_21	72.08	0.09	16.64	0.48	0.12	0.05	2.51	5.43	2.51	0.06	0.02	100	1.68		
	JHT_32	72.40	0.82	14.37	1.47	0.03	0.07	1.71	4.11	4.64	0.10	0.29	100	3.22		
	JHT_17	73.61	0.95	12.46	2.91	0.00	0.43	1.39	3.61	4.44	0.09	0.11	100	4.45		
	JHT_8	73.78	0.29	14.27	1.49	0.15	0.27	1.04	5.08	3.49	0.10	0.03	100	3.83		
	JHT_29	75.63	0.35	13.41	1.12	0.01	0.15	1.58	4.39	3.21	0.09	0.05	100	0.34		
	JHT_6	75.86	0.22	13.76	1.08	0.02	0.28	1.48	3.23	4.00	0.04	0.04	100	2.62		
	JHT_35	76.03	0.26	13.52	1.06	0.07	0.28	1.50	3.65	3.54	0.00	0.09	100	1.89		
	JHT_27	76.19	0.22	13.93	1.15	0.00	0.35	1.43	2.64	3.99	0.02	0.08	100	2.69		
	JHT_18	76.77	0.29	12.33	1.37	0.08	0.24	0.79	3.07	5.03	0.03	0.00	100	3.05		
	JHT_1	77.11	0.23	13.05	0.71	0.11	0.27	1.02	3.68	3.65	0.04	0.14	100	4.33		
	JHT_23	77.62	0.09	12.80	1.06	0.06	0.05	0.36	3.87	3.97	0.08	0.04	100	4.26		
	JHT_19	77.94	0.64	11.74	1.38	0.03	0.14	0.67	3.40	3.95	0.03	0.09	100	4.17		
	Mean	72.13	0.72	14.07	2.46	0.06	0.52	2.05	4.03	3.71	0.08	0.17	100	2.95	25	Heterogeneous tephra
	STDEV	3.84	0.47	1.27	1.56	0.05	0.54	1.10	0.72	0.73	0.04	0.13	0	1.26		
RS126																
	RS126_3	70.38	0.49	15.30	2.34	0.19	0.55	1.82	5.49	3.06	0.27	0.10	100	0.41		
	RS126_6	70.61	0.53	15.32	2.37	0.24	0.43	1.77	5.44	2.84	0.31	0.13	100	1.78		
	RS126_20	70.66	0.54	15.47	2.28	0.11	0.43	1.74	5.43	2.87	0.36	0.09	100	4.86		
	RS126_11	70.78	0.48	15.16	2.22	0.20	0.48	1.67	5.50	3.14	0.27	0.11	100	1.76		
	RS126_17	70.87	0.50	15.08	2.35	0.14	0.51	1.74	5.44	3.02	0.26	0.10	100	1.28		
	RS126_19	71.15	0.54	15.31	2.17	0.02	0.50	1.77	4.98	3.17	0.29	0.08	100	5.32		
	RS126_13	72.19	0.50	15.43	2.49	0.23	0.50	1.74	3.60	3.00	0.25	0.07	100	2.18		

	RS126_8	72.26	0.51	15.40	2.44	0.12	0.51	1.93	3.41	3.05	0.27	0.11	100	1.83		
	RS126_24	72.62	0.53	15.30	2.49	0.08	0.48	1.85	3.26	3.01	0.26	0.12	100	3.44		
	Mean	71.28	0.51	15.31	2.35	0.15	0.49	1.78	4.73	3.02	0.28	0.10	100	2.54	9	Aniakchak CFE II correlative
	STDEV	0.84	0.02	0.12	0.11	0.07	0.04	0.08	1.00	0.11	0.03	0.02	0	1.65		
WBP 65																
	WBP65_1	70.52	0.46	15.26	2.34	0.09	0.53	1.78	5.70	2.98	0.29	0.05	100	2.47		
	WBP65_18	70.62	0.48	15.37	2.45	0.10	0.49	1.70	5.32	3.10	0.31	0.07	100	3.27		
	WBP65_13	70.65	0.50	15.26	2.34	0.06	0.55	1.71	5.57	3.00	0.24	0.10	100	1.79		
	WBP65_12	70.68	0.48	15.09	2.20	0.13	0.47	1.74	5.77	3.08	0.30	0.06	100	0.72		
	WBP65_14	70.75	0.51	15.04	2.18	0.09	0.51	1.69	5.72	3.06	0.33	0.12	100	5.44		
	WBP65_10	70.77	0.53	15.09	2.23	0.16	0.51	1.61	5.91	2.90	0.22	0.07	100	1.72		
	WBP65_6	70.81	0.47	15.27	2.16	0.06	0.48	1.73	5.65	3.03	0.26	0.07	100	0.66		
	WBP65_11	70.84	0.50	15.09	2.35	0.06	0.52	1.77	5.55	2.93	0.31	0.09	100	3.67		
	Mean	70.71	0.49	15.18	2.28	0.09	0.51	1.72	5.65	3.01	0.28	0.08	100	2.47	8	Aniakchak CFE II correlative
	STDEV	0.11	0.02	0.12	0.10	0.03	0.02	0.05	0.17	0.07	0.04	0.02	0	1.61		

Table S3: Secondary standard data accompanying EPMA glass analyses.

Oxford secondary standards (MPI-DING reference glasses, Jochum *et al.,* 2006)

Tephra	Sample	SiO_2	TiO2	Al_2O_3	FeO_T	MnO	MgO	CaO	Na_2O	K_2O	P_2O_5	Cl	Total
StHs6180-G													
	StHs6180-G_1	63.11	0.68	17.62	4.34	0.02	1.91	5.20	4.79	1.28	0.03	0.01	98.98
	StHs6180-G_2	63.78	0.67	17.70	4.55	0.14	1.92	5.34	4.69	1.35	0.09	0.00	100.22
	StHs6180-G_3	63.95	0.76	17.84	4.55	0.03	1.98	5.27	4.85	1.29	0.08	0.00	100.61
	StHs6180-G_4	63.93	0.68	17.72	4.13	0.11	1.82	5.48	4.96	1.34	0.15	0.02	100.35
	StHs6180-G_5	64.04	0.70	17.69	4.20	0.01	1.94	5.34	4.93	1.25	0.11	0.01	100.22
	StHs6180-G_6	64.04	0.66	17.73	4.35	0.10	1.93	5.25	4.30	1.28	0.10	0.01	99.75
	Mean	63.81	0.69	17.72	4.35	0.07	1.92	5.31	4.75	1.30	0.09	0.01	100.02
	STDEV	0.36	0.04	0.07	0.17	0.05	0.05	0.10	0.24	0.04	0.04	0.01	0.58
ATHO-G													
	ATHO-G_3	74.86	0.27	12.15	3.17	0.16	0.10	1.65	4.12	2.66	0.02	0.01	99.17
	ATHO-G_4	75.42	0.23	12.16	3.10	0.17	0.09	1.73	4.22	2.76	0.02	0.03	99.93
	ATHO-G_5	75.19	0.29	12.11	3.19	0.13	0.11	1.74	4.08	2.78	0.03	0.03	99.67
	ATHO-G_6	74.73	0.20	12.11	3.37	0.08	0.08	1.69	4.34	2.77	0.01	0.04	99.42
	Mean	75.05	0.25	12.13	3.21	0.14	0.09	1.70	4.19	2.74	0.02	0.03	99.55
	STDEV	0.32	0.04	0.03	0.12	0.04	0.01	0.04	0.11	0.06	0.01	0.01	0.33
GOR132-G													
	GOR132-G_1	45.21	0.33	11.05	10.17	0.11	22.17	8.70	0.91	0.03	0.04	0.01	98.73
	GOR132-G_2	44.98	0.30	10.93	10.29	0.10	22.14	8.58	0.88	0.04	0.04	0.00	98.28
	GOR132-G_3	45.58	0.33	11.08	10.49	0.22	22.28	8.40	0.87	0.04	0.03	0.01	99.34
	GOR132-G_4	45.38	0.29	11.03	9.77	0.06	22.21	8.52	0.83	0.04	0.04	0.00	98.17
	GOR132-G_5	45.52	0.25	11.07	10.23	0.17	22.06	8.64	0.70	0.04	0.02	0.00	98.70
	GOR132-G_6	45.37	0.28	11.10	10.49	0.19	22.11	8.56	0.75	0.02	0.06	0.01	98.92

Mean	45.34	0.30	11.04	10.24	0.14	22.16	8.57	0.82	0.03	0.04	0.01	98.69
STDEV	0.22	0.03	0.06	0.27	0.06	0.08	0.10	0.08	0.01	0.01	0.01	0.43

Alberta secondary standards

Tephra	Sample	SiO_2	TiO2	Al_2O_3	FeO_T	MnO	MgO	CaO	Na_2O	K_2O	Cl	Total
Lipari												
	ID3506 test	74.03	0.02	13.12	1.57	0.06	0.04	0.59	4.04	5.01	0.48	98.85
	ID3506 test2	74.88	0.09	13.32	1.56	0.08	0.05	0.64	3.95	5.32	0.31	100.13
	ID3506 test3	74.45	0.08	13.27	1.50	0.06	0.05	0.61	4.07	5.16	0.28	99.47
	ID3506_1	74.41	0.10	13.25	1.55	0.02	0.03	0.61	4.04	5.12	0.34	99.40
	ID3506_2	74.16	0.06	13.01	1.52	0.05	0.03	0.64	3.94	5.05	0.36	98.75
	ID3506_3	74.81	0.06	13.37	1.52	0.05	0.03	0.68	4.02	5.11	0.29	99.88
	ID3506_4	73.72	0.10	13.12	1.56	0.02	0.05	0.61	4.12	5.11	0.35	98.68
	ID3506_5	74.18	0.08	13.45	1.65	0.00	0.03	0.61	4.00	5.10	0.31	99.33
	ID3506_6	74.22	0.10	13.21	1.59	0.10	0.05	0.64	4.04	5.11	0.35	99.33
	ID3506_7	73.49	0.06	13.06	1.52	0.06	0.03	0.54	4.19	5.08	0.35	98.31
	ID3506_8	74.63	0.06	13.10	1.68	0.04	0.03	0.55	4.02	5.26	0.30	99.61
	ID3506_9	74.18	0.05	13.36	1.46	0.00	0.04	0.55	3.95	5.14	0.36	99.01
	ID3506_10	74.32	0.11	13.20	1.53	0.06	0.04	0.54	4.09	5.11	0.36	99.28
	ID3506_11	74.46	0.02	13.30	1.60	0.06	0.06	0.54	4.09	5.07	0.32	99.44
	ID3506_12	74.80	0.09	13.14	1.58	0.05	0.06	0.54	3.90	5.17	0.33	99.59
	ID3506_13	73.09	0.08	13.00	1.55	0.06	0.05	0.48	3.99	5.09	0.31	97.63
	ID3506_14	73.53	0.10	13.08	1.50	0.06	0.03	0.52	3.90	5.08	0.38	98.10
	ID3506_15	73.35	0.05	12.97	1.54	0.07	0.05	0.43	3.98	5.09	0.33	97.79
	ID3506_16	73.52	0.09	12.98	1.56	0.02	0.04	0.49	3.83	5.11	0.35	97.91

ID3506_17	74.24	0.09	13.08	1.46	0.09	0.05	0.48	4.17	4.98	0.35	98.91
ID3506_18	73.54	0.05	13.24	1.56	0.05	0.04	0.49	4.15	5.13	0.35	98.53
ID3506_19	74.14	0.08	13.10	1.54	0.05	0.04	0.51	3.89	5.15	0.34	98.75
ID3506_20	74.26	0.07	13.25	1.53	0.05	0.04	0.52	3.87	5.23	0.35	99.10
ID3506_21	74.06	0.07	13.01	1.60	0.04	0.04	0.51	4.19	5.10	0.35	98.88
ID3506_22	73.57	0.05	13.16	1.53	0.07	0.07	0.48	3.86	5.03	0.33	98.07
ID3506_23	74.00	0.08	13.22	1.46	0.13	0.07	0.49	4.00	5.14	0.32	98.85
ID3056_24	73.93	0.05	13.08	1.59	0.09	0.04	0.52	4.01	5.31	0.35	98.89
ID3506_26	74.42	0.07	13.17	1.57	0.07	0.04	0.54	4.04	5.15	0.34	99.32
ID3506_27	74.55	0.08	13.36	1.61	0.11	0.04	0.48	3.96	4.97	0.33	99.43
ID3506_28	74.60	0.05	13.03	1.56	0.08	0.04	0.50	3.99	5.17	0.38	99.33
ID3506_29	73.85	0.10	12.96	1.58	0.04	0.06	0.46	4.05	5.11	0.34	98.47
ID3506_30	74.00	0.07	13.32	1.69	0.07	0.05	0.54	4.11	5.22	0.30	99.31
Mean	74.11	0.07	13.16	1.56	0.06	0.04	0.54	4.02	5.12	0.34	98.95
STDEV	0.45	0.02	0.13	0.05	0.03	0.01	0.06	0.10	0.08	0.03	0.61
ID3506 Official	74.10	0.07	13.10	1.55	0.07	0.04	0.74	4.06	5.13	0.34	99.09
	0.96	0.03	0.34	0.06	0.03	0.02	0.05	0.28	0.26	0.03	

Old Crow

SK_Old Crow_1	72.36	0.29	12.57	1.62	0.05	0.25	1.25	3.56	3.65	0.23	95.77
SK_Old Crow_2	71.93	0.25	12.70	1.51	0.12	0.27	1.20	3.45	3.54	0.28	95.18
SK_Old Crow_3	73.21	0.32	12.83	1.58	0.07	0.26	1.19	3.82	3.42	0.27	96.90
SK_Old Crow_4	71.71	0.29	12.48	1.65	0.04	0.24	1.18	3.54	3.52	0.23	94.84
SK_Old Crow_5	71.86	0.33	12.64	1.61	0.08	0.25	1.18	3.55	3.43	0.25	95.13
SK_Old Crow_6	72.64	0.26	12.55	1.62	0.06	0.28	1.28	3.80	3.47	0.25	96.16

SK_Old Crow_7	72.33	0.26	12.54	1.61	0.06	0.27	1.10	3.81	3.51	0.26	95.70
SK_Old Crow_8	70.82	0.25	12.55	1.62	0.06	0.25	0.98	5.02	3.68	0.21	95.39
SK_Old Crow_9	71.76	0.27	12.55	1.58	0.05	0.26	1.11	3.48	3.67	0.29	94.94
SK_Old Crow_10	71.89	0.28	12.60	1.66	0.09	0.28	1.09	3.57	3.74	0.29	95.43
SK_Old Crow_11	74.21	0.30	12.84	1.71	0.05	0.28	1.09	3.68	3.68	0.26	98.05
SK_Old Crow_12	71.16	0.28	12.49	1.61	0.13	0.24	1.01	3.46	3.49	0.24	94.05
SK_Old Crow_13	73.63	0.36	13.05	1.59	0.09	0.27	0.99	3.82	3.59	0.27	97.60
SK_Old Crow_14	71.68	0.23	12.48	1.62	0.01	0.26	0.98	3.83	3.50	0.27	94.80
SK_Old Crow_15	72.98	0.33	12.70	1.62	0.06	0.30	1.00	3.77	3.65	0.25	96.59
SK_Old Crow_16	71.73	0.23	12.34	1.61	0.07	0.28	1.01	3.40	3.70	0.27	94.58
SK_Old Crow_17	72.14	0.29	12.37	1.66	0.02	0.29	0.97	3.71	3.63	0.24	95.26
SK_Old Crow_18	72.68	0.23	12.71	1.59	0.04	0.28	0.97	3.81	3.49	0.27	96.00
SK_Old Crow_19	73.84	0.33	12.57	1.66	0.07	0.28	1.07	2.81	3.67	0.26	96.49
SK_Old Crow_20	72.52	0.29	12.61	1.65	0.02	0.26	1.01	3.66	3.57	0.28	95.79
SK_Old Crow_21	71.80	0.31	12.50	1.56	0.11	0.28	1.01	3.37	3.56	0.28	94.70
SK_Old Crow_22	71.87	0.22	12.44	1.55	0.03	0.26	1.03	3.33	3.48	0.28	94.42
SK_Old Crow_23	71.55	0.26	12.85	1.62	0.08	0.25	1.03	3.77	3.70	0.24	95.29
SK_Old Crow_24	71.56	0.34	12.43	1.62	0.12	0.27	1.04	3.74	3.64	0.25	94.96
SK_Old Crow_25	71.73	0.33	12.51	1.62	0.05	0.30	1.00	3.64	3.71	0.28	95.11
SK_Old Crow_26	71.78	0.26	12.48	1.60	0.03	0.25	0.97	3.49	3.70	0.24	94.75
SK_Old Crow_27	71.09	0.25	12.14	1.53	0.00	0.31	0.90	3.34	3.52	0.22	93.24
SK_Old Crow_28	71.28	0.30	12.30	1.64	0.12	0.29	0.99	3.49	3.68	0.21	94.25
SK_Old Crow_29	71.09	0.30	12.39	1.55	0.03	0.23	0.92	3.54	3.52	0.23	93.75
SK_Old Crow_30	71.49	0.38	12.43	1.55	0.09	0.25	0.90	3.51	3.45	0.25	94.24
SK_Old Crow_31	73.56	0.22	12.74	1.61	0.03	0.27	1.00	3.93	3.56	0.26	97.10
Mean	72.16	0.29	12.57	1.61	0.06	0.27	1.05	3.65	3.59	0.26	95.44

STDEV	0.85	0.04	0.17	0.04	0.03	0.02	0.10	0.34	0.10	0.02	1.05
Old Crow Offical	71.90	0.30	12.57	1.63	0.05	0.28	1.42	3.67	3.56	0.27	95.68
	1.00	0.05	0.34	0.14	0.03	0.03	0.05	0.26	0.26	0.05	

Table S4: Radiocarbon dates used in the construction of age models within this study.

Radiocarbon dates produced as part of the Lakes and the Arctic Carbon Cycle project (LAC) (NERC ref NE/K000233/1).

Site	Laboratory Number	Depth (cm)	14C Age	error	Material	Note
Jan Lake	SUERC-50484	132.5	4204	37	Twig fragment	
Jan Lake	SUERC-50485	190.5	8867	41	Five *Potamogeton* cf natans seeds	
Woody Bottom Pond	SUERC-58893	33.5	1750	35	terrestrial wood fragment	
Woody Bottom Pond	UCIAMS-154532	63	3605	30	*Carex* seed, beetle fragment, wood fragment	
Woody Bottom Pond	SUERC-58895	107.5	4175	37	bark of shrub (willow?)	
Woody Bottom Pond	UCIAMS-154535	138.5	5100	30	*Potamogeton* seeds	
Woody Bottom Pond	UCIAMS-170261	150	5680	25	*Typha*/*Phragmites* stem, insect chitin, charcoal, rhizomes	
Woody Bottom Pond	UCIAMS-172053	167.5	5450	35	terrestrial plant and insect fragments	Rejected (too young)
Woody Bottom Pond	SUERC-63546	186.5	8000	39	Twig	
Woody Bottom Pond	SUERC-50486	198.5	8564	40	*Nuphar lutea* seed	
Ruppert Central	UCIAMS-139067	43.5	6125	35	*Carex* nut, deciduous leaf and twig fragments, charredplant fragments	Rejected (too old)
Ruppert Central	UCIAMS-154508	100.5	2200	25	Terrestrial plant leaf	
Ruppert Central	UCIAMS-164425	145	4635	25	One Betulaceae, one *Betula* fruit; *Betula* bud scale; terr leaf frags	
Ruppert Central	UCIAMS-139068	165.5	5790	35	grass stem frags, cf *Picea* needle	
Ruppert Central	UCIAMS-154509	177	6250	30	terrestrial plant material	
Ruppert Central	SUERC-58892	195	8806	43	Twig	
Ruppert Central	UCIAMS-164417	216	7760	70	Rhizomes, insect wing, *Populus* catkin bract, fruits: one Betulaceae, three *Betula nana*, one *Betula*	
Ruppert Central	UCIAMS-154510	224	8145	35	terrestrial plant fragments	
Ruppert Central	UCIAMS-164418	240	8650	60	*Betula nana* fruit, fragments of: cf *Andromeda, Vaccinium, Myrica gale* leaf	
Ruppert Central	UCIAMS-154529	278.5	10500	70	*Nuphar* or terrestrial	

Ruppert Central	SUERC-50487	284.5	13837	59	mostly twiggy fragments, leaf frags	
Ruppert Central	UCIAMS-172052	326.5	12290	260	terrestrial plant and insect fragments	
Ruppert Central	UCIAMS-154527	361	13410	270	pieces of wood on caddisfly larval case	
Ruppert Side	UCIAMS-172054	89.5	2530	45	bud scale	
Ruppert Side	UCIAMS-172056	104.5	2910	35	half conifer needle	
Ruppert Side	UCIAMS-172057	150.5	3560	25	Twig, *Betula* fruit, seed	
Ruppert Side	UCIAMS-172058	199.5	5305	20	conifer needle	
Ruppert Side	SUERC-60063	230.5	6281	36	Twig	
Ruppert Side	UCIAMS-172059	267.5	9310	80	bud scale, terrestrial plant fragments	
Ruppert Side	UCIAMS-172060	308.5	11080	90	terrestrial plant or monocot fragments	
Ruppert Side	SUERC-63547	345.5	39341	1085	terrestrial wood fragment	Rejected (too old)
Ruppert Side	UCIAMS-172051	355	13820	130	terrestrial plant and insect fragments	
Ruppert Side	UCIAMS-172061	404	20420	70	terrestrial plant or monocot fragments	

Radiocarbon dates published in Carsonl and Finney, (2004)

Site	Laboratory Number	Depth (cm)	14C Age	error	Material	Note
Jan Lake	CAMS-56435	39-42	1220	50	*Picea* pollen	
Jan Lake	CAMS-56436	89-82	1400	100	Terrestrial macrofossils (one *Picea* needle tip and six *Betula* seeds)	
Jan Lake	CAMS-56437	79-82	1650	50	*Picea* pollen	
Jan Lake	CAMS-48495	101-104	2920	90	*Betula* seed and bract; unidentified peticole	
Jan Lake	CAMS-16065	151-153	4100	50	Aquatic macrofossil	
Jan Lake	CAMS-56438	173-175	5000	110	Terrestrial macrofossils (three *Betula* seeds, one C*arex* seed, one leaf fragment)	
Jan Lake	CAMS-56439	173-175	5220	50	*Picea* pollen	
Jan Lake	CAMS-39079	202-203	6230	100	*Picea* needles and seed	
Jan Lake	CAMS-39080	203-204	6360	90	Unidentified plant fragments	
Jan Lake	CAMS-39081	205-206	6500	100	*Betula* seeds	
Jan Lake	CAMS-56440	212-214	7260	50	Terrestrial macrofossils (two *Alnus* seeds, two *Picea* seeds, two *Picea* seed wing fragments, six leaf fragments.	
Jan Lake	CAMS-56441	212-214	7220	40	Picea pollen	
Jan Lake	CAMS-56442	219-221	7570	100	Terrestrial macrofossils (one *Picea* needle tip, three *Picea* needle fragments, one *Picea* seed wing fragment, one grass seed, one *Carex* seed)	
Jan Lake	CAMS-56443	219-221	8050	50	*Picea* pollen	
Jan Lake	CAMS-39082	226-227	8830	50	*Potamogeton* seeds	
Jan Lake	CAMS-48496	272-273	11590	100	Moss fragments	Rejected (too old)
Jan Lake	CAMS-48497	298-301	5220	150	Unidentified plant fragments	Rejected (too young)
Jan Lake	CAMS-56444	299-301	22180	140	Pollen	Rejected (too old)
Jan Lake	CAMS-56445	301-303	10010	60	Pollen	
Jan Lake	CAMS-16066	344-346	12220	70	Wood	
Jan Lake	CAMS-58299	364-365	12410	50	Unidentified plant fragments	
Jan Lake	CAMS-48498	364-365	12430	40	*Salix* twig	

Table S5: Additional diagrams referred to in the text

Figure 1: Bivariate plots of major and minor element glass chemistry from Jan Lake and Brooks Range tephras, probed at the University of Oxford and the University of Alberta.

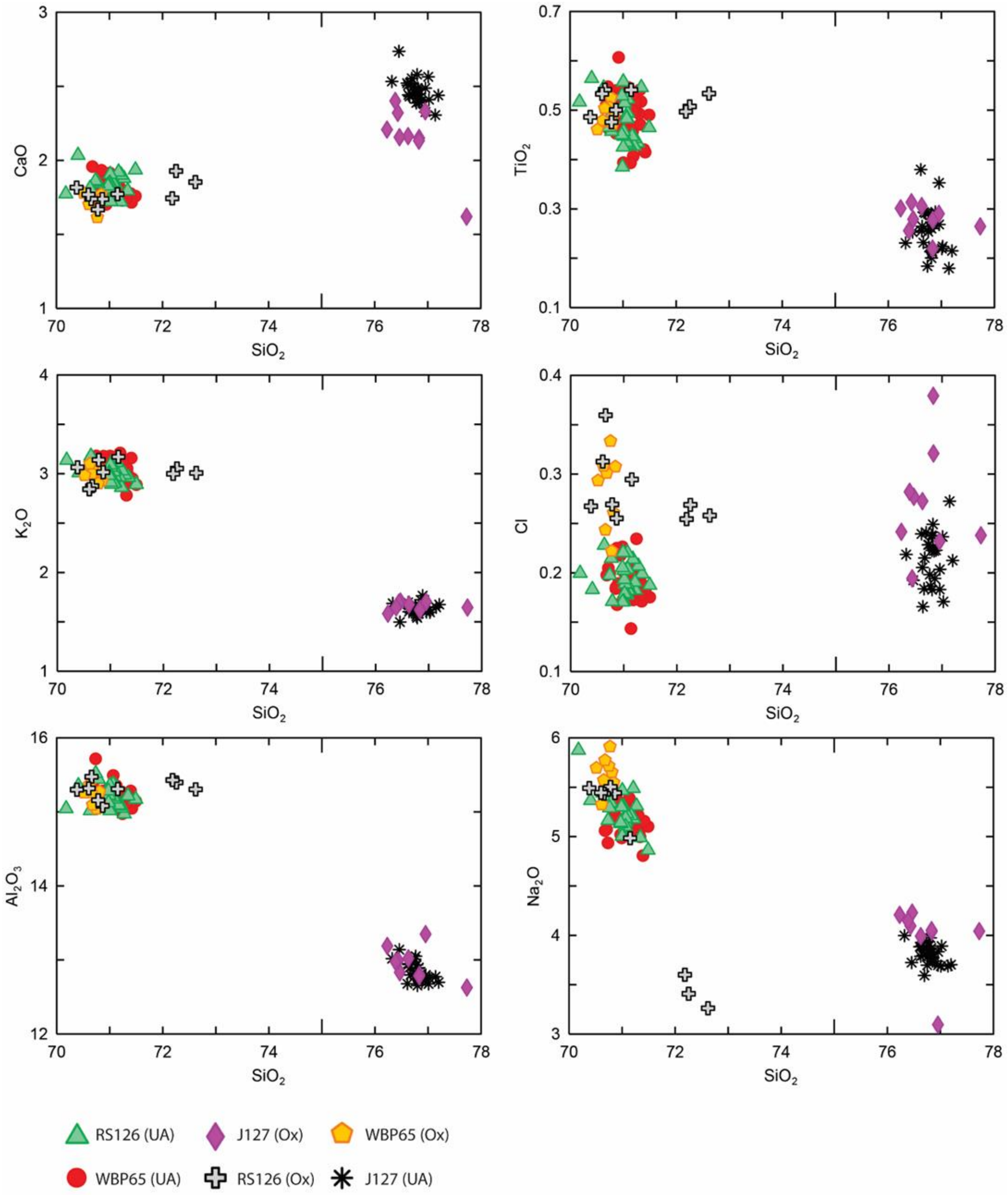

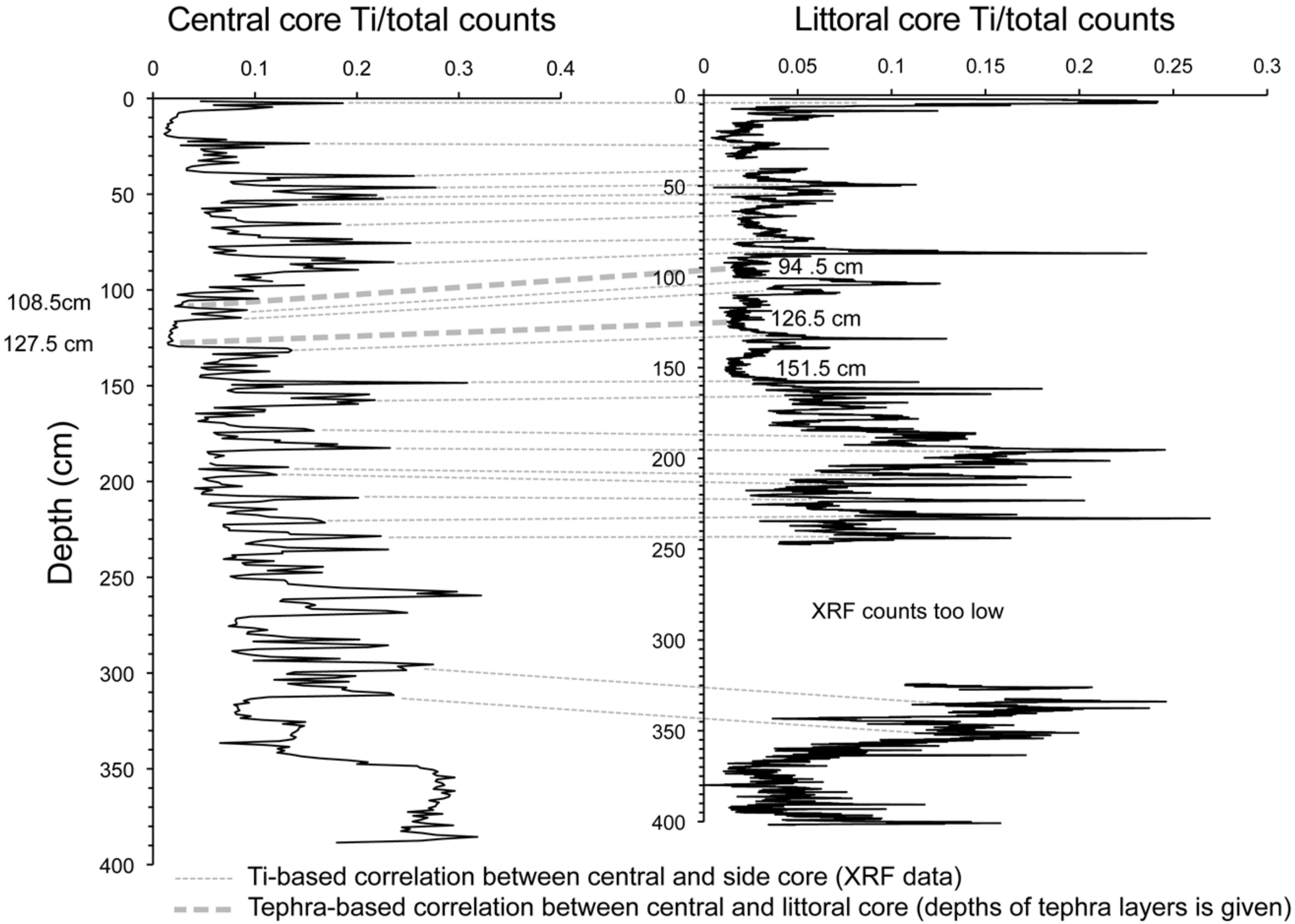

Figure 2: Titanium values used in the correlation of clay bands between RS and RC.

Table S6: Additional References

Jochum, K.P., Stoll, B., Herwig, K., Willbold, M., Hofmann, A.W., Amini, M., Aarburg, S., Abouchami, W., Hellebrand, E., Mocek, B., Raczek, I., 2006. MPI-DING reference glasses for in situ microanalysis: New reference values for element concentrations and isotope ratios. Geochemistry, Geophysics, Geosystems, 7(2).

Figure Click here to download Figure Figure 1 (greyscale).tif

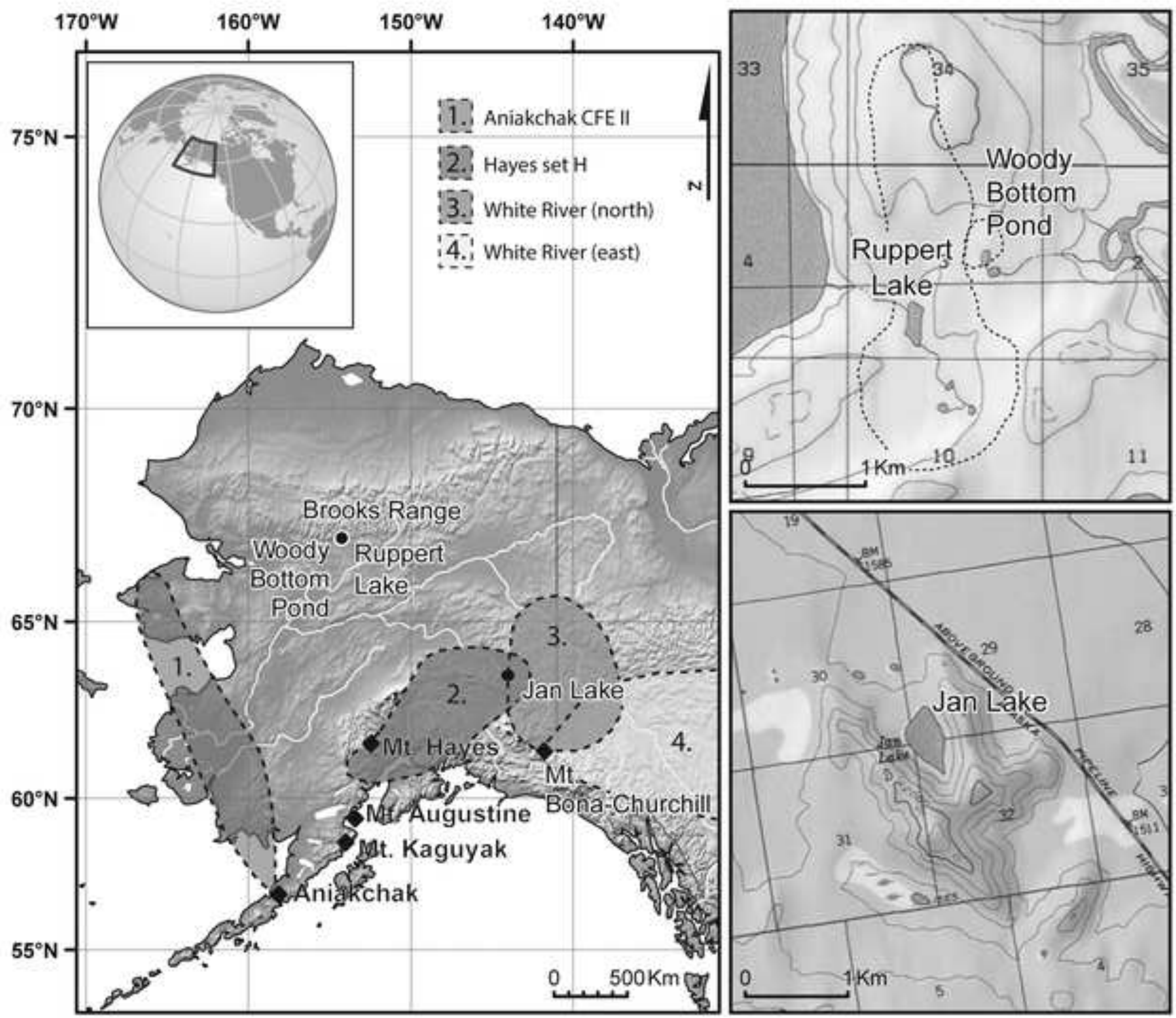

Figure

Click here to download Figure Figure 1 Colour.tif

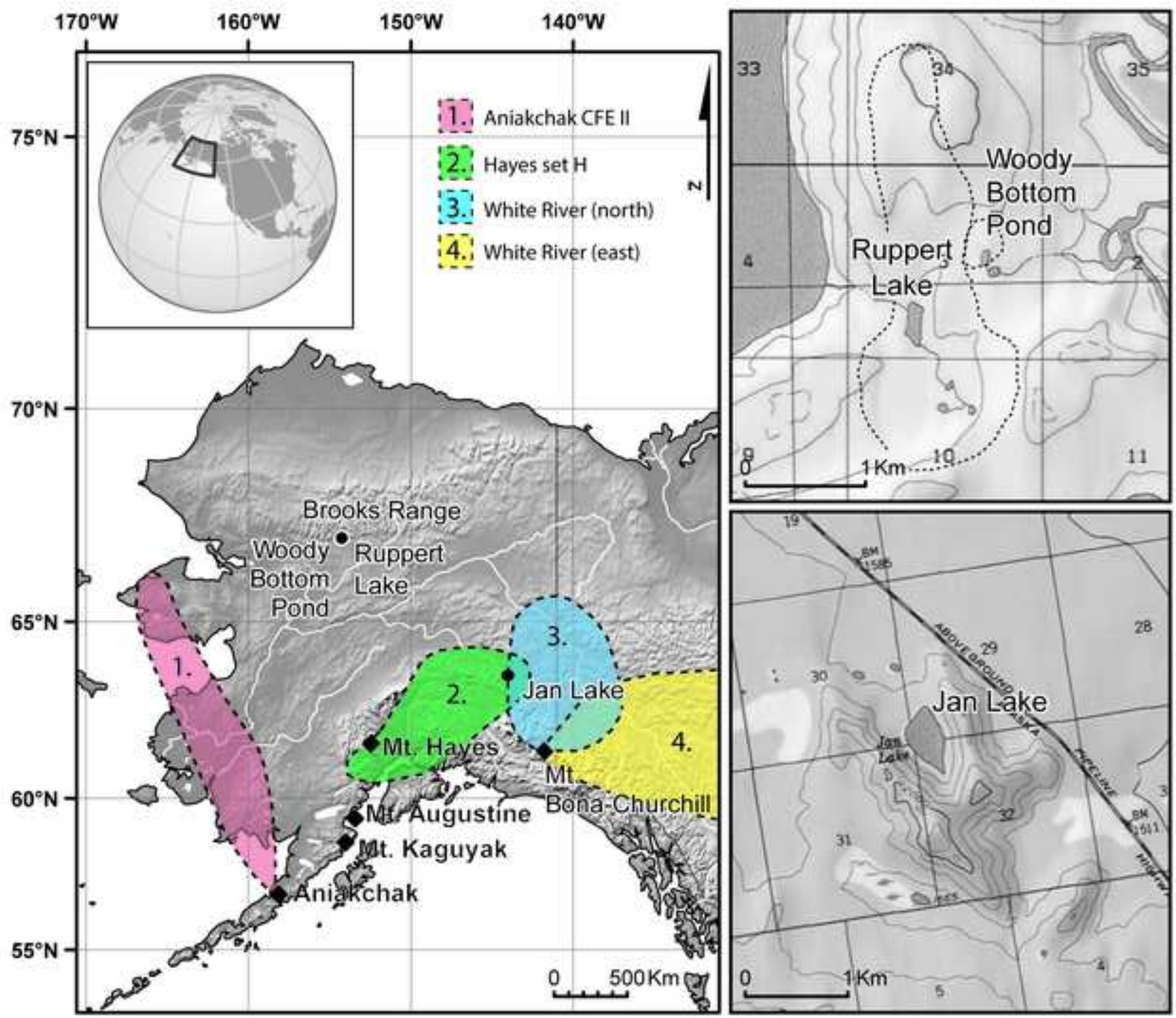

Figure

Click here to download Figure Figure 2.tif

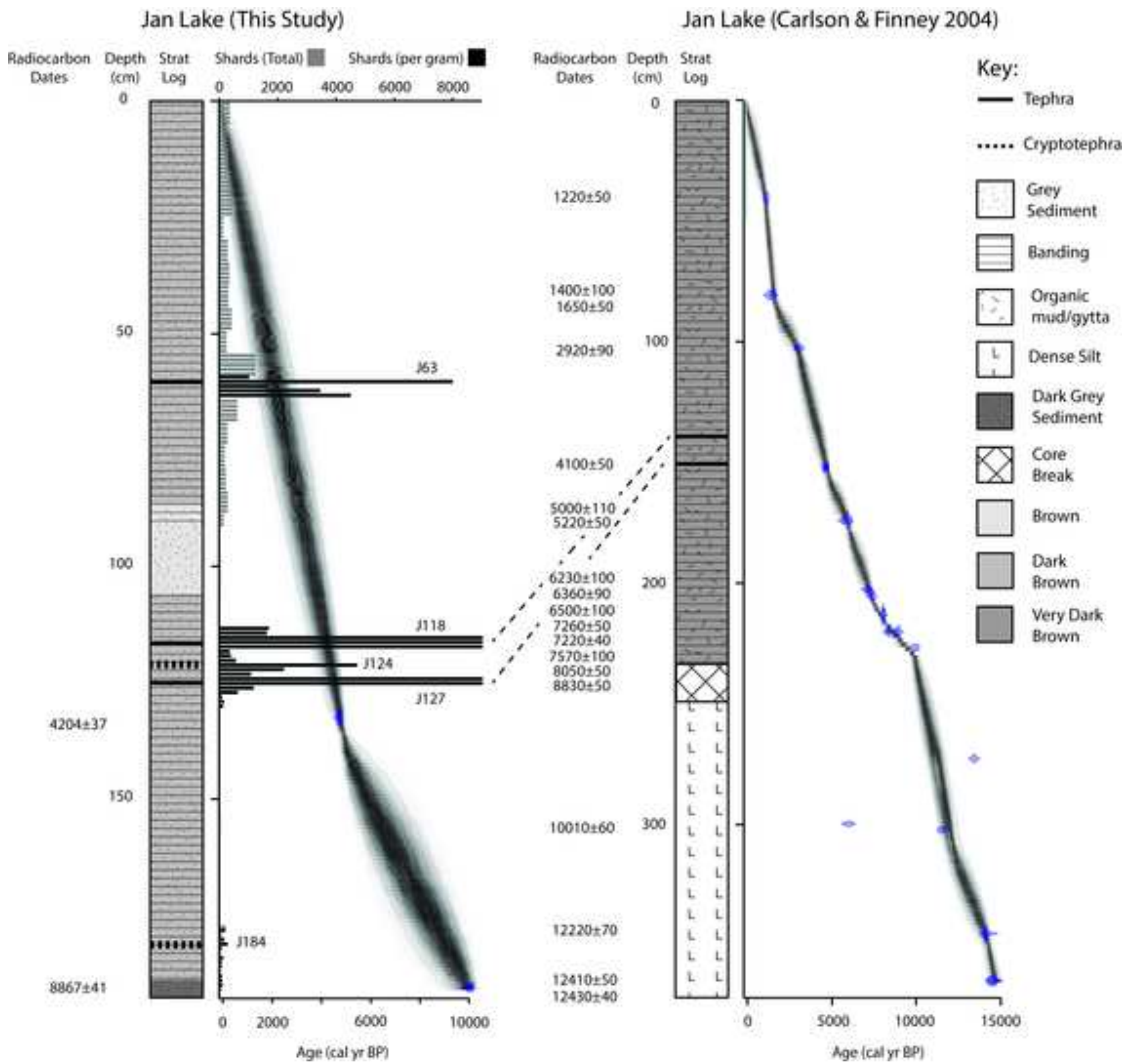

Figure

Click here to download Figure Figure 4.tif

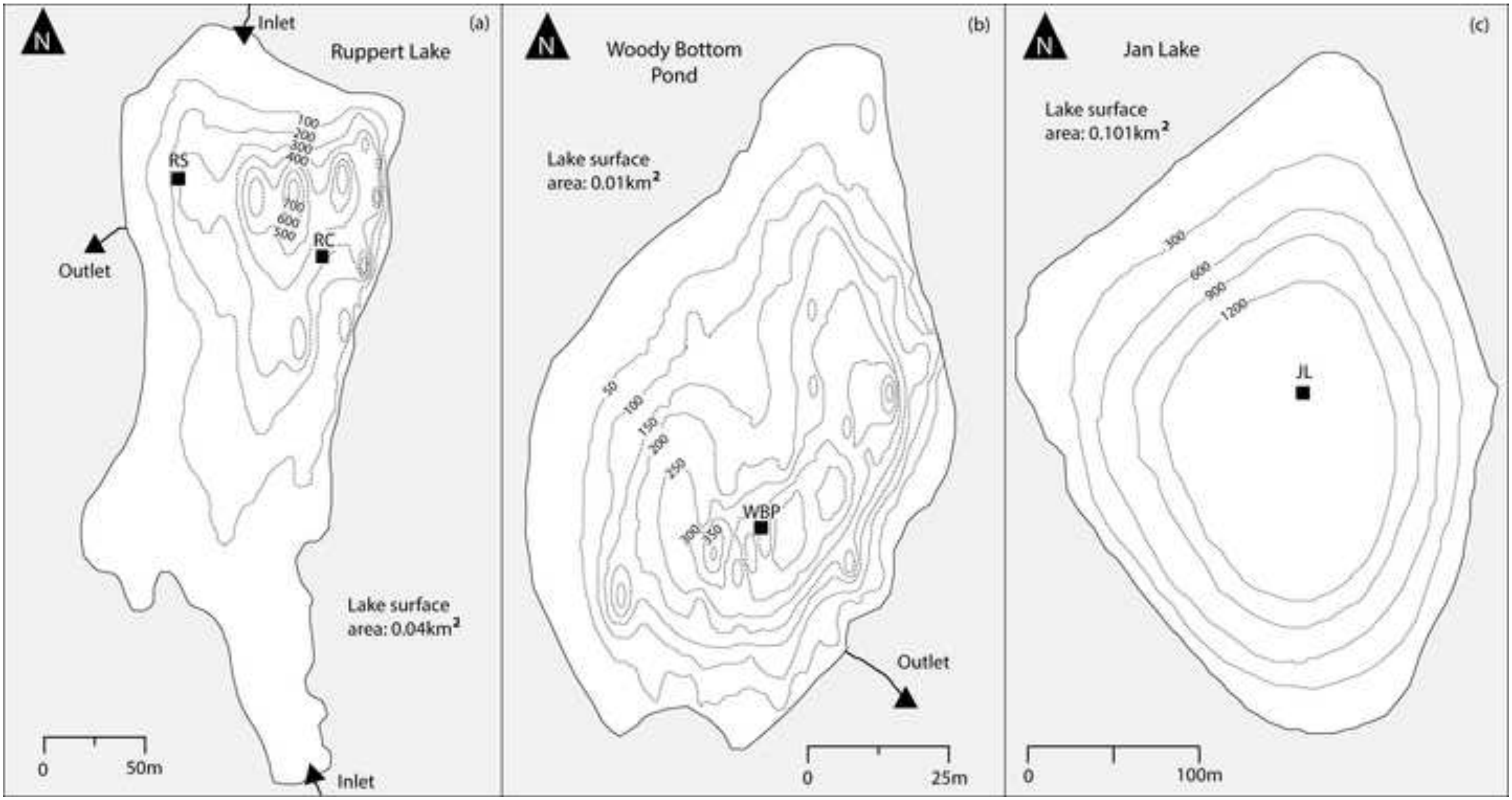

Figure

Click here to download Figure Figure 5.tif